SULFONAMIDE PARTITIONING TO AQUEOUS CATIONIC MICELLAR SYSTEMS

by

Patrick J. Cashin

A thesis submitted to the Department of Chemistry

In conformity with the requirements for

the degree of Master of Science

Queen's University

Kingston, Ontario, Canada

(January, 2011)

Abstract

Advances in analytical chemistry have resulted in a growing body of literature showing measurable concentrations of pharmaceuticals in both drinking and wastewater. Removal of such chemicals is typically inefficient and often poorly characterized. To characterize one such method of removal (micellar enhanced ultrafiltration, (MEUF)), interactions of a cetyl trimethylammonium bromide (CTABr) surfactant and sulfonamide antibiotics were examined by NMR and semi-equilibrium dialysis (SED).

The locus and orientation of binding in a micelle was established for seven sulfonamides by ^{1}H NMR, and it was found that hydrophilic sulfonamides showed weak coordination with the micelle, whereas hydrophobic sulfonamides penetrated into the micellar interior with coordination of the SO_2NH group to the charged surface layer.

Binding constants were determined by ^{1}H NMR and showed apparent order of magnitude differences between nuclei. Several compounds were unable to be characterized in this manner due to low change in chemical shift with addition of CTABr. SED was performed as an alternative method to determine binding constants. Values determined in this manner were higher than those determined by ^{1}H NMR. Binding constants were converted into changes in Gibbs free energy and used to evaluate and, where necessary, modify the orientation and locus proposed by ^{1}H NMR.

Attempts are made to correlate binding constants with octanol-water partition coefficients to determine if a free energy relationship can be derived. Characterization of these systems may allow for a predictive methodology to determine the MEUF removal efficiencies of new sulfonamide and surfactant combinations. It is also hoped that this work may be generalized to predict MEUF efficiency for a wide range of contaminants that might be found in wastewater.

Acknowledgements

I would first like to thank my supervisors, Dr. R. Stephen Brown and Dr. Erwin Buncel, whose knowledge and encouragement were invaluable. Also, my thanks to Dr. Richard Oleschuk and Dr. Gary vanLoon for sitting as members of my supervisory committee.

In addition to my supervisors, I also had many other advisors during the production of this thesis. My thanks go out first to Dr. Julian M. Dust (visiting Professor from Grenfell Campus, Memorial University of Newfoundland), who has now played an immense role in two of my theses to date. Also, my thanks to Dr. Vimal Balakrishnan and Dr. Kirsten Exall of Environment Canada, whose advice and recommendations played a huge role in the direction this thesis took.

Thanks to all the members of the Brown group, and in particular two undergraduate students who I had the pleasure of working with, Hilary Chung and Bradley Taylor. Also, a huge thank you to my fellow Musketeers, Jonathan Byer and Elize Ceschia. Between the three of us, we somehow managed to maintain our mutual sanity during grad school!

For funding, I would like to thank Environment Canada and Queen's University. I would also like to thank Environment Canada for the use of their facilities.

Finally, thanks to my family and friends for their support and encouragement, without which I may never have left home, but which welcomed me back whenever I needed a rest.

Table of Contents

List of Figures

List of Tables

List of Abbreviations

^{1}H NMR – Proton Nuclear Magnetic Resonance

CTABr – Cetyl Trimethylammonium Bromide

LC-MS/MS – Liquid Chromatography-Triple Quadrupole Mass Spectrometry

MEUF – Micellar Enhanced Ultrafiltration

MWCO – Molecular Weight Cutoff

SED – Semi-equilibrium Dialysis

WWTP – Wastewater Treatment Plant

Chapter 1

Introduction

1.1 General Introduction

Sulfonamide antibiotics (compounds containing the SO_2NH functional group shown below which exhibit antibiotic properties) have been synthesized for

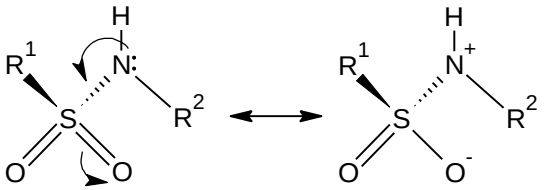

over one hundred years, with p-aminobenzenesulfonamide (or sulfanilamide, Figure 1.1) having been first synthesized in 1908 during dye stuff research[1].Despite extensive attempts at characterization of this compound, it was not until the mid-1930's that the antibiotic properties of a sulfanilamide derivative, sulfamidochrysoidine (commonly known as Prontosil, Figure 1.1) were discovered[2].

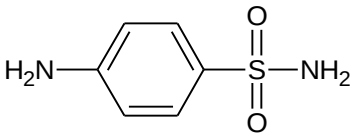

A

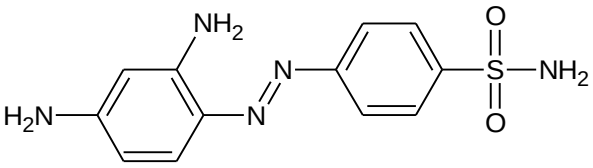

B

Figure 1.1 Structures of A) Sulfanilamide, and B) Prontosil

It was eventually determined that sulfanilamide itself possessed antibiotic properties, however it took many years to become apparent, as such sulfonamides were not utilized fully as antibiotics for some time. Sulfonamides

possess antibiotic properties owing to their similarity to p-aminobenzoic acid, whereby they act as structural analogs to inhibit the production of dihydrofolic acid by dihydropteroate synthase. Reduced dihydrofolic acid synthesis results in the death of various forms of bacteria which are unable to otherwise extract sufficient amounts of folic acid from the environment for their survival[3].

Once the utility of sulfonamides was realized, the medical community began using them extensively until penicillin mass production began in the early 1940's. Penicillin has a much greater utility, as the bacteria did not develop antibiotic resistance to penicillin as quickly when compared to the sulfonamides on the market at the time[4]. Thus, sulfonamides quickly were relegated to more specific uses and to use in less developed countries, in which they still flourish today.

In modern times, various pharmaceuticals are still in use which contain the sulfonamide functionality. The World Health Organization (WHO) lists multiple sulfonamides as essential medicines[5], as shown below.

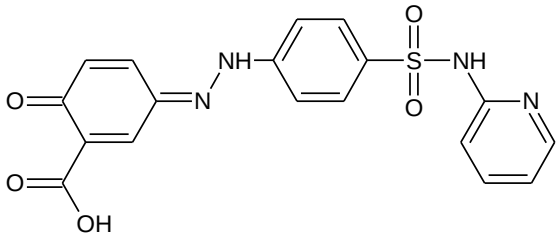

Sulfasalazine

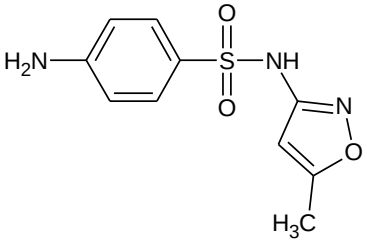

Sulfamethoxazole

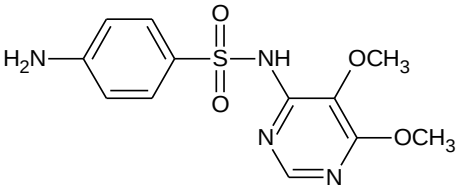

Sulfadoxine

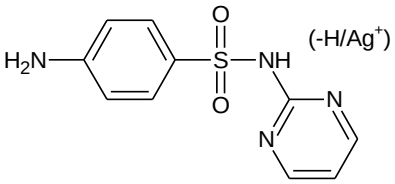

Sulfadiazine (Silver Sulfadiazine)

Figure 1.2 Various Sulfonamides Identified by the WHO as Essential Medicines[5]

The synthesis of sulfonamides is relatively straightforward, with reaction of the corresponding sulfonyl chloride and amine under basic condition to afford the desired product[6].

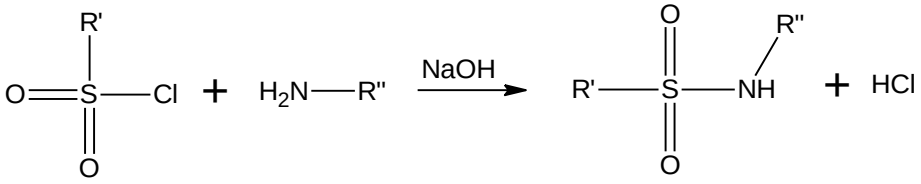

Figure 1.3 Synthesis of Sulfonamides via HCl Condensation

1.2 Sulfonamide Contaminants in the Environment

Despite the extensive history of sulfonamide usage, their behavior in the environment is still poorly characterized. Various analogs can have extremely different solubility and octanol-water partition coefficients (log(K_{OW}).

Sulfaguanidine, bearing a guanidinium moiety as the R^{II} as shown in Figure 1.3 has an extremely high solubility and low log(K_{OW}) of -1.22, whereas sulfamethazine has instead a dimethylpyrimidine and a log(K_{OW}) of 0.89[7]. Since many sulfonamides also contain groups that are protonated or deprotonated easily, it is not expected that they will bioaccumulate to a large extent, and instead their presence in the environment will be limited to how quickly they degrade.

Studies have shown extensively varying degradation properties. Sulfamethoxazole is known to undergo photolytic degradation in water, however varying conditions (distilled water vs. sea water) have had major impacts on the rate, ranging from 98% degradation in distilled water within 30 minutes to 14% degradation in 7 hours in sea water[8]. Thus, degradation behavior is highly unpredictable, and has not been systematically studied for any large number of sulfonamides.

Multiple sulfonamides have been found in consistently low but measurable concentrations in water, and the results of two studies can be found below in Table 1.1. While sources such as farming and aquaculture are of particular interest in the case of veterinary antibiotics[9], human sources are also prevalent. They, however, are more likely to be point sources such as sewer outfalls.

Table 1.1 Concentration of Sulfonamide Detected in Various Matrices

Compound	Reference	Matrix	Concentration (Median, ppb)
Sulfamethoxazole	10	WWTP Influent	0.25
Sulfamethoxazole	10	WWTP Effluent	0.05
Sulfamethoxazole	11	River	0.14
Sulfasalazine	10	WWTP Influent	Non-Detect
Sulfasalazine	10	WWTP Effluent	0.04

Given the prevalence of these antibiotics and their poorly understood degradation behavior, increasing incidences of bacterial resistance to antibiotics, and potential human effects of small doses over a long period of time, removing such antibiotics from water is a growing concern.

1.3 Sulfonamide Removal from Wastewater

Wastewater treatment is comprised of three stages – primary, secondary, and tertiary treatment. Primary treatment generally consists of allowing the various solid particulates in water to settle or be filtered out, either from the use of settling tanks or a series of progressively smaller filters[12]. Thus, removal of sulfonamides by primary treatment is limited to the amount of sulfonamide that is partitioned to the solid matter in wastewater that is filtered, and is typically small since sulfonamides are too hydrophilic to partition greatly to sediment. Use of very small filtration membranes to perform reverse osmosis and nanofiltration, while effective, is typically not performed as the volume of water to be treated would make costs prohibitively high, the costs being inversely proportional to pore size.

Secondary treatment involves reduction of the organic content of water by allowing for microorganism growth on some sort of medium, in the process significantly reducing the dissolved organic content of water[12]. In this case, sulfonamides will be removed only as much as the organism layer, that the water is in contact with, will degrade the sulfonamide.

Tertiary treatment holds the greatest promise for the removal of sulfonamides, being designed to purify water for reuse. Activated carbon and sand filtration in this phase may remove some amount of sulfonamide, however studies have shown that removal of sulfonamides by wastewater treatment plants is often ineffective at best. It has been shown that sand filtration can show removal of up to 80% for compounds which have a $\log(K_{OW}) > 3$, however for compounds with $\log(K_{OW}) < 3$, removal efficiencies greater than 50% are not expected by this method[13]. As with partitioning to sediments removed in primary treatment, sulfonamides are too hydrophilic to be removed in this manner.

Experiments conducted with powdered activated carbon showed attenuation of some sulfonamides at concentrations approaching 1 ppm; others were removed to only a small degree. Sulfonamides such as sulfamerazine and sulfamethazine showed removal efficiencies ranging from 86-~100%, analogs such as sulfamethoxazole and sulfathiazole showed removal efficiencies of 22-50%[14].

Other tertiary treatment methods are equally ineffective. Advanced oxidation shows some potential, giving good removal efficiencies (<90%) for

selected sulfonamides with ozonolysis, however concentrations of both ozone and sulfonamide were particularly high[15].

1.4 Micellar-Enhanced Ultrafiltration for Sulfonamide Removal

In order to remove sulfonamides from water using filtration, a modified form of standard filtration can be considered. As demonstrated in Figure 1.4[16], any type of filtration with a pore size larger than that employed in nanofiltration would be ineffective for small organic molecules. In this work, a derivative of ultrafiltration known as micellar enhanced ultrafiltration (MEUF) is examined and characterized with respect to the binding sulfonamides to aqueous surfactant micelles.

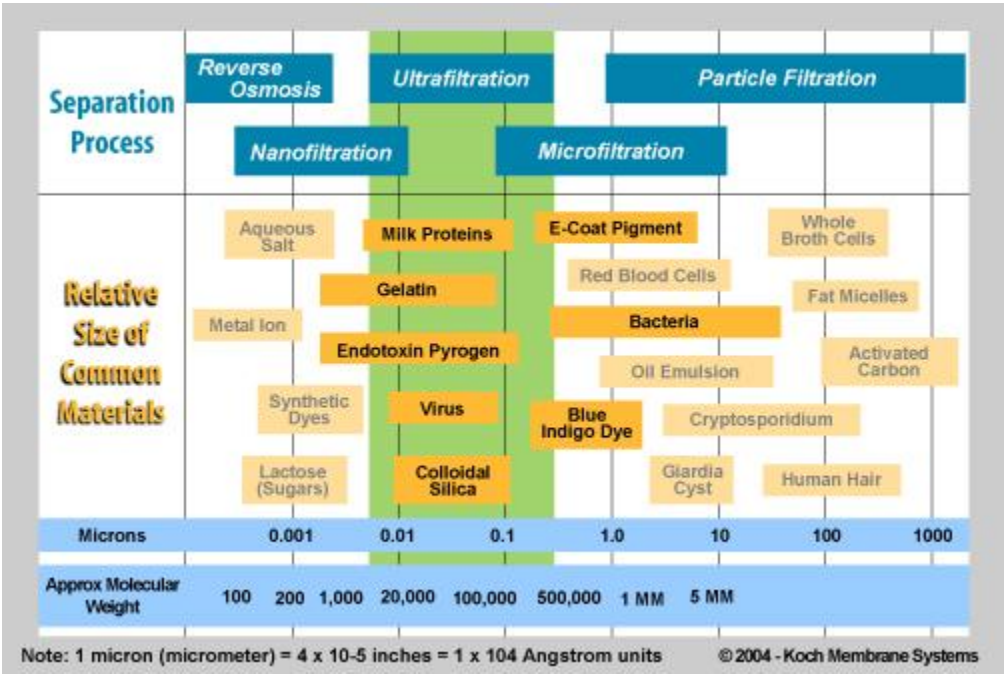

Figure 1.4 Effective Ranges of Filtration Systems

(Taken from Reference 16)

MEUF works on the same basic principles as an ultrafiltration system – a membrane is employed with a pore size such that molecules or aggregates above a certain molecular weight cut-off (MWCO) are not allowed to pass through, resulting in a permeate that is free of species above the MWCO. However, given that a typical MWCO can be between 7,000-20,000 Da, small molecules would not be trapped in the retentate[17].

If a surfactant is employed in the system at above the critical micelle concentration (C_{CMC}), enhanced retention for small molecules is observed. A typical micelle of the cationic surfactant cetyl trimethylammonium bromide (CTABr) can have an aggregation number of over approximately 150 at 50 mM[18], and thus such an aggregate could have, in theory, a mass of over 42,000 Da and so the micelle, along with any species partitioned to it, should be retained in an ultrafiltration system.

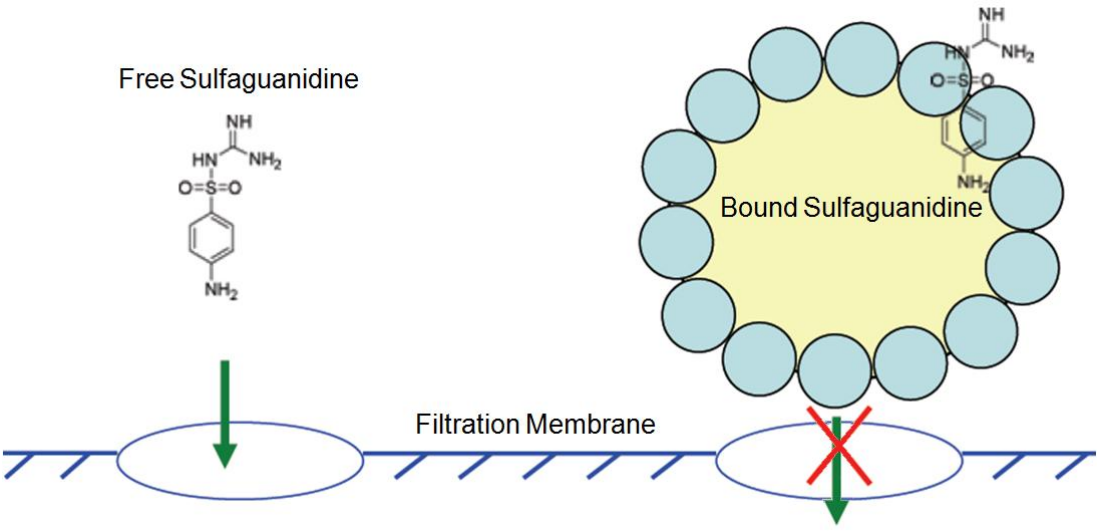

Figure 1.5 Illustration of Removal of Sulfaguanidine via MEUF

Any surfactant could potentially be used for MEUF, provided the aggregates are of a sufficient size to be filtered out by the given membrane. However, given the nature of the molecules being studied, a cationic surfactant would likely be most effective. Anionic and neutral surfactants also exist, with varying molecular weights and C_{CMC}.

In choosing a potential surfactant for MEUF, there are several characteristics that must be examined. Low costs are of importance, particularly in the case of widespread use. Low toxicity is also a factor, as well as a low C_{CMC} - both to reduce the amount of surfactant used, as well as minimize the monomeric form escaping through the membrane.

MEUF systems have been used with both cationic and anionic surfactants to effect the removal of many varied species such as metal cations[19,20], as well as organic contaminants[21,22]. It has been proposed that a MEUF system could be viable for removal of sulfonamide antibiotics, however conditions for removal have yet to be optimized, and the mechanism of action is still somewhat unclear.

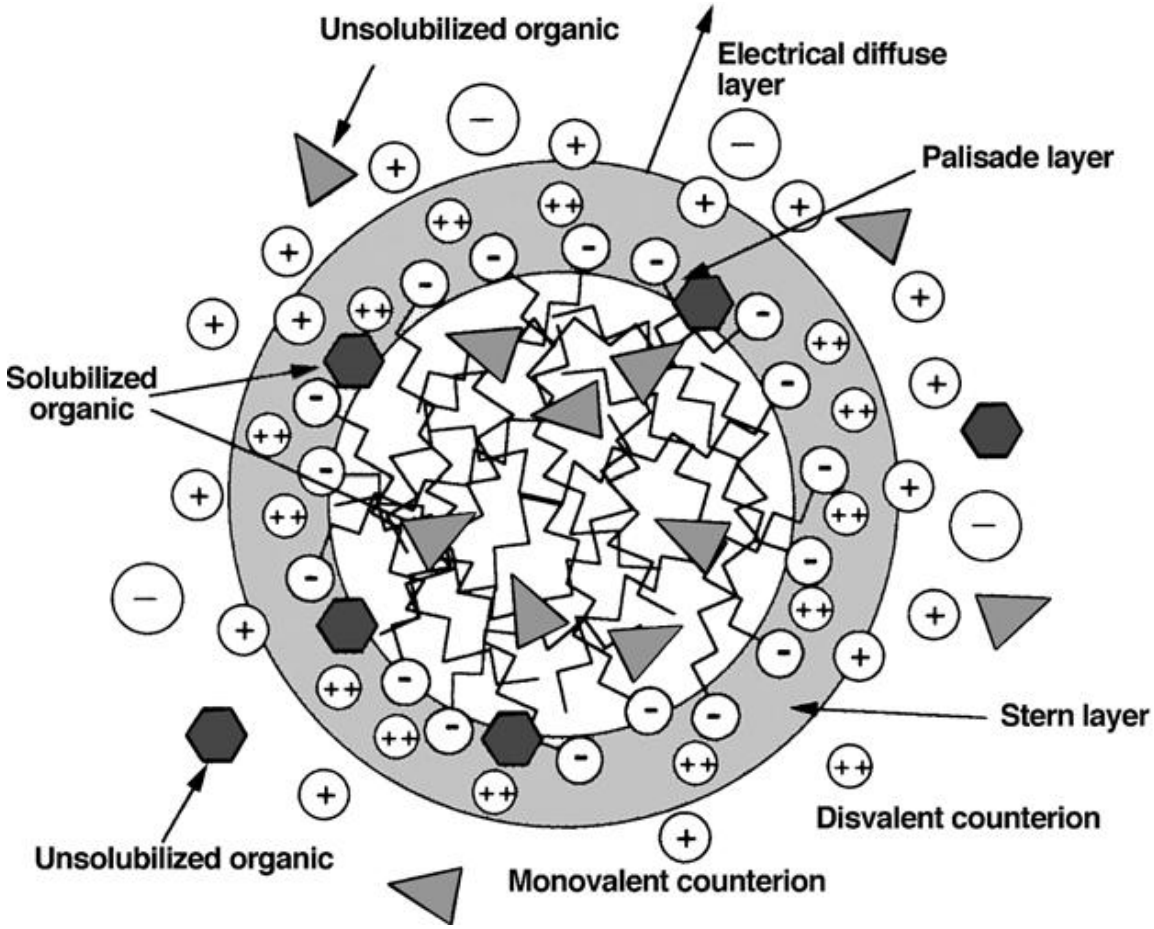

Figure 1.6 Illustration of Contaminant Binding to an Anionic Micelle

(Adapted with permission from Reference 13)

A key parameter that must be considered to perform MEUF is the C_{CMC} of the surfactant being used. Below this concentration, surfactants will exist only in a monomeric form and in small aggregates. Above this concentration, surfactants will form characteristic micelles of various types, such as spheres, rods, or flattened discs[23]. This value of C_{CMC}, however, is quite susceptible to various parameters, such as salinity and buffer concentration[24] and even the use of a deuterated solvent[25].

Determination of the C_{CMC} of a surfactant can be done in many ways. Common physical properties include conductivity, interfacial tension, surface tension, and osmotic pressure[23]. Other techniques utilize the use of a probe molecule such as benzoylacetone, which undergoes a keto-enol tautomerization, the position of which is shifted by the existence of a micelle[26]. This, however, has the unfortunate side effect of affecting the C_{CMC}, and so when used the concentration of the probe molecule must be kept low, and if possible, the values checked against other methods.

In order to characterize this system, it is necessary to understand how a molecule is able to bind with a micellar substrate. Once we can be sure that the concentration of surfactant in solution is above the C_{CMC}, to perform MEUF, the contaminant of interest must partition to the micelle. Contaminants can coordinate with a micelle through multiple methods, such as the hydrophobic effect, cation-anion binding, and ion-dipole interactions. Various literature reports have commented on the interactions and ultrafiltration of dyes and cationic or anionic micelles[27,28], so it is plausible that a sulfonamide antibiotic should partition to a micelle. The exact locus and method of binding will vary with each sulfonamide compound.

The goals of this study are then to characterize the mechanism by which sulfonamides are able to partition to an aqueous micelle of CTABr by determination of a binding constant, and by establishing a qualitative diagram of the orientation and locus of binding of the sulfonamide within the micelle.

1.5 References

(1) Weatherall, M. *In search of a cure : a history of the pharmaceutical industry*; Oxford University Press: Oxford ; New York, 1990.

(2) Sneader, W. *Drug discovery : a history*; Wiley: Hoboken, N.J., 2005.

(3) Bertram, G. K.; Masters, S. B.; Trevor, A. J. *Basic and Clinical Pharmacology (11th Edition)*; McGraw-Hill Professional Publishing: New York, NY, USA, 2009.

(4) *Making Medicines: A brief history of pharmacy and pharmaceuticals*; Anderson, S., Ed.; Pharmaceutical Press, 2005.

(5) W.H.O. 2010.

(6) de Boer, T. J.; Backer, H. J. *J Org Synth* **1964**, *4*.

(7) US National Library of Medicine.

(8) Trovo, A. G.; Nogueira, R. F. P.; Aguera, A.; Sirtori, C.; Fernandez-Alba, A. R. *Chemosphere* **2009**, *77*, 1292.

(9) Lalumera, G. M.; Calamari, D.; Galli, P.; Castiglioni, S.; Crosa, G.; Fanelli, R. *Chemosphere* **2004**, *54*, 661.

(10) Watkinson, A. J.; Murby, E. J.; Kolpin, D. W.; Costanzo, S. D. *Sci Total Environ* **2009**, *407*, 2711.

(11) Xu, W. H.; Zhang, G.; Li, X. D.; Zou, S. C.; Li, P.; Hu, Z. H.; Li, J. *Water Res* **2007**, *41*, 4526.

(12) U.S. Environmental Protection Agency Primer for Municipal Wastewater Treatment Systems http://www.epa.gov/owm (Accessed January 2011)

(13) Nakada, N.; Shinohara, H.; Murata, A.; Kiri, K.; Managaki, S.; Sato, N.; Takada, H. *Water Res* **2007**, *41*, 4373.

(14) Choi, K. J.; Kim, S. G.; Kim, S. H. *Environ. Technol.* **2008**, *29*, 333.

(15) Lin, A. Y.-C.; Lin, C.-F.; Chiou, J.-M.; Hong, P. K. A. *J Hazard Mater* **2009**, *171*, 452

(16) Koch Membrane Systems.

(17) Lemordant, D. In *Encyclopedia of surface and colloid science*; Hubbard, A. T., Ed. 2006, p 4 v.

(18) Aswal, V. K.; Goyal, P. S. *Chem Phys Lett* **2003**, *368*, 59.

(19) Ghezzi, L.; Robinson, B. H.; Secco, F.; Tine, M. R.; Venturini, M. *Colloid Surface A* **2008**, *329*, 12.

(20) Atwood, J. L.; Steed, J. W. *Encyclopedia of supramolecular chemistry*; M. Dekker: New York, 2004.

(21) Zeng, G. M.; Xu, K.; Huang, J. H.; Li, X.; Fang, Y. Y.; Qu, Y. H. *J Membrane Sci* **2008**, *310*, 149.

(22) Purkait, M. K.; DasGupta, S.; De, S. *Sep Purif Technol* **2004**, *37*, 81.

(23) Farn, R. J. *Chemistry and technology of surfactants*; Blackwell Pub.: Oxford ; Ames, Iowa, 2006.

(24) Fuguet, E.; Rafols, C.; Roses, M.; Bosch, E. *Anal Chim Acta* **2005**, *548*, 95.

(25) Emerson, M. F.; Holtzer, A. *J Phys Chem* **1967**, *71*, 3320.

(26) Dominguez, A.; Fernandez, A.; Gonzalez, N.; Iglesias, E.; Montenegro, L. *J Chem Educ* **1997**, *74*, 1227.

(27) Zaghbani, N.; Hafiane, A.; Dhahbi, M. *Sep Purif Technol* **2007**, *55*, 117.

(28) Zaghbani, N.; Hafiane, A.; Dhahbi, M. *Desalination* **2008**, *222*, 348.

Chapter 2

^{1}H NMR and UV-Vis Characterization

2.1 Introduction

Understanding the solubilization of antibiotics into aqueous micellar systems requires an *in situ* measurement technique to determine binding characteristics. Nuclear magnetic resonance (NMR) spectroscopy studies provide a potentially useful technique whereby the environment of specific atoms can be probed *in situ* to determine the locus and orientation of a solubilized molecule within a micelle[1-8].

Previous literature reports by Farias et al. indicate that polar molecules such as sulfonamide antibiotics should be located close to the charged layer of a cationic micelle[3]. They, however, examined only a single sulfonamide antibiotic, sulfamethoxazole. It is of interest to characterize a set of eight sulfonamide antibiotic in the cationic surfactant cetyl trimethylammonium bromide (CTABr).

A wealth of literature exists on binding constants and micellar solubilization; however, relatively few publications examine specifically micellar binding constants as determined by NMR studies[9,10]. Thus, it was of interest to determine a method by which the binding locus and orientation, and an overall micellar binding constant, could be determined by ^{1}H NMR.

To determine via NMR if a molecule is being solubilized by a micelle, we can examine possible changes in the chemical shift (δ) of the solubilized molecule resulting from a change in the environment of the molecule.

Nuclear magnetic resonance is a technique by which the connectivity and electronic structure of a molecule can be non-destructively probed. If we consider the case of ^{1}H NMR, a proton has a spin I = 1/2. This implies that when such a proton is placed into a magnetic field, it will generate two different energy states, corresponding to the spin up (m_1 = +1/2) and spin down (m_1 = -1/2) spin potential of the atom. These states will line up parallel to the applied magnetic field in the case of spin up situation, or antiparallel to the applied magnetic field for the spin down situation. The energy of these two states is non-equivalent, and can be calculated as shown in Figure 2.1.

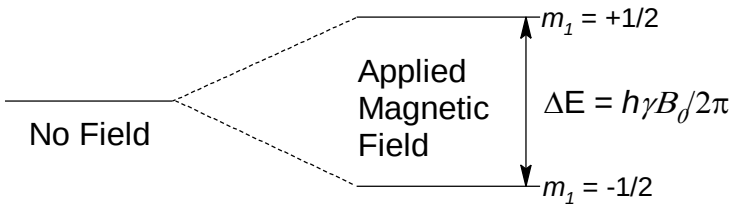

Figure 2.1 Energy Difference Between Electron Spin States in a Magnetic Field

Where γ is the gyromagnetic ratio (γ = 1 for hydrogen); and

B_0 is the strength of the magnetic field.

The energy difference between the two will result in an uneven distribution which can be described by the Boltzmann equation, Equation 2.1:

$$\frac{N_\beta}{N_\alpha} = e^{\frac{-\Delta E}{kT}}$$

Equation 2.1 Boltzmann Equation for the Population of Two Energy States

Where N_β is the population of the high energy spin down state; and

N_α is the population of the low energy spin up state.

In order to ascertain any useable information from this system, the next step is to somehow perturb it. This is performed by applying a second magnetic field which oscillates at an appropriate radio frequency, the application time of which is sufficient to shift the orientation of the nucleus, from parallel with the original magnetic field; to an appropriate angle (in the case of ^{1}H NMR, often 90°). At this point, the nucleus will then return to the stable configuration due to the force exerted by being out of alignment with the applied field. To return to its stable configuration, the nucleus will rotate about the axis of the applied magnetic field in a manner known as Larmor precession until it returns to the stable configuration. By measuring this decay via the current induced in a coil and applying a Fourier Transform to the data, we are able to produce an NMR spectrum. The chemical shift then is a direct measure of the energy difference between the two spin states.

If we consider a proton again, however this time one in a different electronic environment, we should see a change in the chemical shift. When a sample is put into a magnetic field, the applied magnetic field will result in an induced magnetic field due to the electrons of the atom which will counteract the

applied magnetic field. In the case of an electron deficient atom, this induced magnetic field will be weaker, and so the atom is said to be deshielded, resulting in a greater energy difference between the spin up and down states. As such, the atom will be affected more by the applied magnetic field and the frequency of its precession back to normal will increase, and so the chemical shift for the atom will also increase. Similarly, an atom in an electron rich environment will be shielded from the applied magnetic field, the energy difference will decrease, and so the frequency of precession and consequent chemical shift will decrease.

Chemical shifts are often measured relative to the hydrogen present in tetramethylsilane, $(CH_3)_4Si$, which is assigned a chemical shift of $\delta = 0$ ppm. Since measurements of chemical shift are actually measurements of the electronic environment of an atom, any change in chemical shift implies a change in the environment. Shifts downfield are commonly associated with a more electron poor environment, whereas upfield shifts indicate relatively electron rich environments.

The above approach of correlating direction of change of chemical shift with changes in the electronic environment has been used to determine the solubilization environment of various chemicals. From ^1H NMR chemical shifts, Farias et al. were able to determine that sulfamethoxazole, when partitioned into benzalkonium chloride, was located in the headgroup region of the micelle. Metronidazole, a nitroimidazole derivative, was determined to be located near the

surface of the micelle, with a weak interaction, as shown by the small ^{1}H NMR chemical shift changes observed.

Similar studies by Xu et al. examined the solubilization of phenol and phenoxide by cetylpyridinium chloride and found that phenol partitioned into the headgroup region as well. After addition of a large amount of phenol, some phenol molecules were found deeper in the micelle, but even then very few entered the micellar interior, indicating a preference for the charged layer. Phenoxide partitioned similarly, however it also coordinated with the $C_5H_5N^+$ headgroup. The authors also noted the strong effect of CO_3^{2-}, as increasing concentrations resulted in a lower amount of phenoxide partitioned into the micelle due to CO_3^{2-} competing with the phenoxide for binding to the charged $C_5H_5N^+$ groups[8]. This would seem to indicate different types of binding depending on the charge state of the phenol/phenoxide pair. For neutral species, hydrophobic effects and pi-cation effects dominate, whereas the negatively charged species location is affected more by ion-ion type interactions, which can be decreased by the introduction of a competing anion.

To fully characterize the system, two different NMR chemical shift curves must be examined: 1) The change in chemical shift of the sulfonamide protons at constant sulfonamide concentration with varying surfactant concentration, and 2) Surfactant protons at constant surfactant concentration with varying sulfonamide concentration.

Interactions between micelles and sulfonamides occur fast on the NMR time scale, and thus the spectrum is an average of the environments experienced by all the components of surfactant-sulfonamide system. It is thus possible that the same data that gives us the location of a sulfonamide within the micelle can be quantitatively analyzed to give some form of partition or binding constant[11]. Such an equation would require several components, and has been developed, Equation 2.2. Appendix B demonstrates the derivation.

$$\delta = \frac{\delta_0 + \delta_M K_B M_V (C_S - C_{CMC})}{1 + K_B M_V (C_S - C_{CMC})}$$

Equation 2.2 Relation of NMR Chemical Shift and Binding Constant

Where δ is the chemical shift of the proton at C_S;

δ_0 is the initial chemical shift of the proton when C_S = 0;

δ_M is the chemical shift of the proton in a fully bound state;

K_B is the binding constant;

M_V is the molar volume of the surfactant;

C_S is the total concentration of the surfactant; and

C_{CMC} is the critical micelle concentration of the surfactant

A derivation such as the one used to create Equation 2.2 assumes fast exchange on the NMR time scale. This implies that any exchange that occurs between free and bound sulfonamide molecules occurs quickly enough that the chemical shift observed is an average of the two states[11]. In the event of slow

exchange, two separate peaks would be seen, one corresponding to each of the bound and unbound states. Since this is not found, we can assume fast exchange, and the chemical shift is taken to be the weighted average of the two chemical shifts, δ_0 and δ_M.

The use of NMR to determine binding constants is quite widespread, and the manner in which it can be used is quite versatile[12]. An early example is the work of Carper et al. to determine binding constants for fast exchange donor-acceptor complexes of trinitrobenzene with various sulfides and sulfoxides in a series of chlorinated solvents, as well as in carbon disulfide by the use of a Scatchard type plot[13]. Similar studies have been performed previously in the Buncel group on multiple occasions. Binding constants between trinitrobenzene and N,N-dimethylaminoethyl-3,4-dimethoxybenzene were determined by Dust[14]. More recently, binding constants for the association of chlorinated ethylene and β-cyclodextrins have been determined[15]. Also of particular interest from the group is work on degradation of pesticides as catalyzed by micellar systems, where orientations of fenitrothion within a micelle were also determined[16].

2.2 Experimental

2.2.1 Materials

Sulfacetamide, sulfanilamide, sulfadiazine, sulfaguanidine, sulfamerazine, sulfamethazine, sulfamethoxazole, and sulfathiazole (Structures shown below in Table 2.1) were purchased from Sigma-Aldrich Chemicals (Oakville, ON) at the highest grade available and were used without purification. Sulfonamides were selected due to either their availability, or inclusion on the WHO List of Essential Medicines[17]. Cetyl trimethylammonium bromide (CTABr) was also purchased from Sigma-Aldrich Chemicals of the highest grade available, and was used without purification. Benzoylacetone (BZA) was purchased from Sigma-Aldrich Chemicals and used without purification.

All solutions prepared in D_2O were made from D_2O purchased from either Cambridge Isotope Laboratories (Andover, US), or from CDN Isotopes (Pointe-Claire, QC). Deionized water was obtained by using a Milli-Q system (Millipore). Acetonitrile-d_3, ethanol-d_6, methanol-d_4, and DMSO-d_6 were purchased from Cambridge Isotope Laboratories. 1,4-Dioxane was purchased from Fisher Scientific.

Table 2.1 Physical and Chemical Constants for Studied Sulfonamides

Sulfonamide	Structure	Molecular Weight ($g \cdot mol^{-1}$)	pK_{a1}, pK_{a2}[18-22]	$\log(K_{OW})$[23]
Sulfacetamide (1)	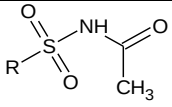	214.24	1.26, 5.32	-0.96
Sulfanilamide (2)	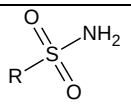	172.20	1.78, 11.19	-0.62
Sulfadiazine (3)	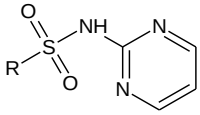	250.28	1.64, 6.50	-0.09
Sulfaguanidine (4)	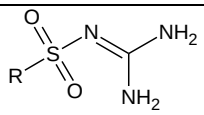	214.24	2.25, 11.69	-1.22
Sulfamerazine (5)	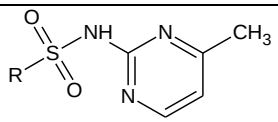	264.31	1.95, 7.45	0.14
Sulfamethazine (6)	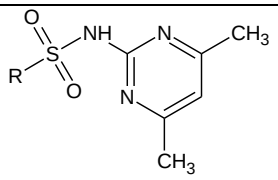	278.33	1.30, 6.21	0.89
Sulfamethoxazole (7)	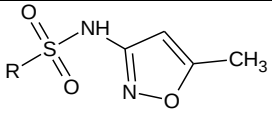	253.28	1.85, 5.60	0.89
Sulfathiazole (8)	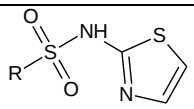	255.32	2.01, 7.11	0.05

Notes:

R = 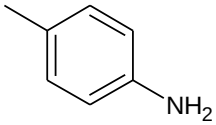

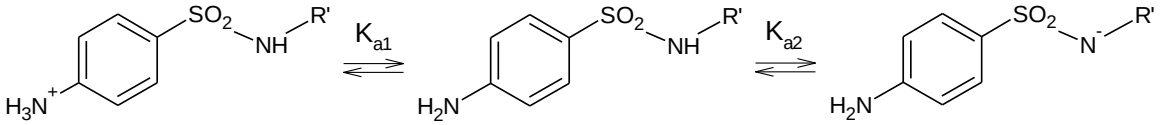

2.2.2 Solution Preparation for NMR Analysis

Standard solutions of sulfonamides used for NMR analysis were prepared from a stock solution made by addition of the appropriate amount of sulfonamide in 25 mL D_2O, followed by sonication at 35°C to aid dissolution. Samples were sonicated again prior to use.

Table 2.2 Sulfonamide Solution Preparation for NMR

Sulfonamide	Mass Added (g)	Amount Added (mol)	Molarity (M)
1	0.0041	$1.9x10^{-5}$	$5.8x10^{-4}$
2	0.0019	$1.1x10^{-5}$	$4.4x10^{-4}$
3	0.0034	$1.4x10^{-5}$	$5.4x10^{-4}$
4	0.0036	$1.7x10^{-5}$	$6.7x10^{-4}$
5	0.0050	$1.9x10^{-5}$	$7.6x10^{-4}$
6	0.0034	$1.2x10^{-5}$	$4.9x10^{-4}$
7	0.0061	$2.4x10^{-5}$	$9.6x10^{-4}$
8	0.0052	$2.0x10^{-5}$	$8.2x10^{-4}$

CTABr solutions were prepared via serial dissolution of a $2.00x10^{-2}$ M CTABr stock solution prepared by dissolving 0.7289 g of CTABr (MW = 364.45 $g•mol^{-1}$) in 100 mL D_2O. Dissolution was aided by placing the solution in an ultrasonic bath at 35°C for 30 minutes. Prior to further use, CTABr stock solutions were sonicated again, as a precipitate would often form if solutions were left at room temperature for a period of longer than one day.

2.2.3 Preparation of Solutions for UV-Vis Analysis

Standard solutions of sulfonamides used for UV-Vis analysis were prepared from a stock solution made by addition of the appropriate amount of sulfonamide in 250 mL H_2O, followed by sonication at 35°C to aid dissolution. Samples were sonicated again prior to use.

Table 2.3 Sulfonamide Solution Preparation for UV-Vis

Sulfonamide	Molecular Weight ($g \cdot mol^{-1}$)	Mass Added (g)	Amount Added (mol)	Molarity (M)
4	214.24	0.0270	1.26×10^{-4}	5.04×10^{-4}
5	264.31	0.0335	1.27×10^{-4}	5.07×10^{-4}
7	253.28	0.0310	1.22×10^{-4}	4.90×10^{-4}
8	255.32	0.0327	1.28×10^{-4}	5.12×10^{-4}

Standard solutions of sulfonamides being used for D_2O studies were prepared similarly.

CTABr solutions were prepared via serial dissolution of a 3.58×10^{-2} M CTABr stock solution prepared by dissolving 1.3116 g of CTABr (MW = 364.45 $g \cdot mol^{-1}$) in 100 mL H_2O or D_2O. Dissolution was aided by placing the solution in an ultrasonic bath at 35°C for 30 minutes. Prior to further use, CTABr stock solutions were sonicated again, as a precipitate would often form if solutions were left at room temperature for a period of longer than one day.

BZA solutions were prepared from a 3.29×10^{-2} M BZA (MW = 134.19 $g \cdot mol^{-1}$) stock solution in 1,4-dioxane. Serial dilutions were performed using deionized water or D_2O.

For UV-Vis analysis of surfactant solutions, BZA solutions were prepared by diluting 1,4-dioxane stock solutions in H_2O or D_2O so that the final concentration was approximately 0.7 mM. Sulfonamide concentrations were held between 2-4 mM, while CTABr concentrations were varied from 0.1 mM to 10 mM.

Final solutions were sonicated prior to analysis, and approximately 0.5 mL of sample placed into standard 5 mm NMR tubes immediately prior to analysis. For samples undergoing UV-Vis analysis, the samples were also prepared at least one day before analysis.

2.2.4 ^{1}H NMR Spectroscopy

All samples were analyzed on a Bruker 500 MHz NMR spectrometer operating at 499.54 MHz with a digital resolution of 0.18 Hz. Samples were all dissolved in D_2O, and chemical shifts (δ) were measured relative to the HOD peak present at approximately δ = 4.8 ppm (samples were held at 298.0K +/- 0.1K to ensure that the HOD peak remained at a constant position). Samples were sonicated prior to analysis and placed in 5 mm NMR tubes. For experiments involving external standards, these standards were prepared in flame sealed capillary tubes which were then placed into the sample to ensure that the addition of standard did not affect the sample.

Spectra were generated quantitatively as the average of 64 individual scans using a 45° pulse of 7.5 μs with a relaxation time (t_1) of 2.7 s. A total of three different experiments were performed for each concentration pairing and

the results averaged, with Δδ for any one concentration being less than 0.002 ppm. When an experiment was broken into two separate NMR sessions, a common concentration was analyzed during each session and used to normalize the data.

The NMR spectrum of CTABr was monitored as the concentration of sulfonamide was varied, and the NMR spectrum of the sulfonamide was monitored as the concentration of CTABr was varied. Assigned NMR spectra can be found in Appendix A, and a representative example of the change noted in the various protons of a sulfonamide, sulfadiazine, with increasing [CTABr] found below in Figure 2.2.

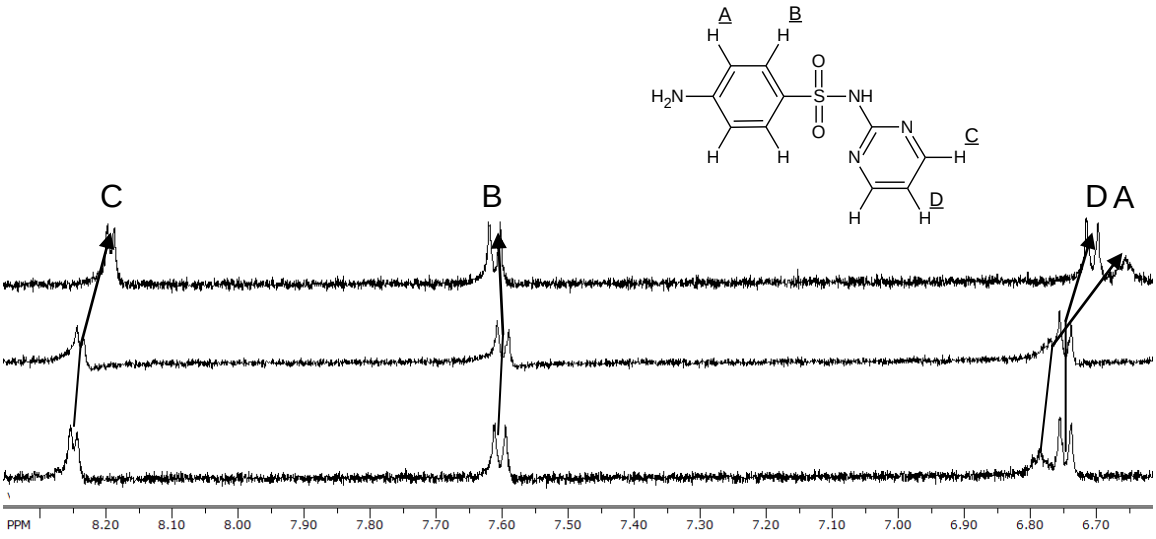

Figure 2.2 Effect of Increasing [CTABr] on the ^{1}H NMR Spectrum of Sulfadiazine

NMR tubes were cleaned with water, methanol, and dichloromethane following use, then left to dry for 24h in an oven at 105°C prior to reuse.

2.2.5 UV-Vis Spectroscopy

All UV-Vis spectra were generated by analyzing solutions relative to a blank of H_2O or D_2O in a matched quartz cuvette. Spectra were generated from 200-800 nm by an Ocean Optics USB4000 Detector using both deuterium and tungsten lamps as a light source. A pathlength of 1.0 cm was used for the cell, with a scan rate of 0.8 sec/spectrum and a spectral bandwidth of 0.22 nm. All spectra were acquired at room temperature (22°C).

Spectra of benzoylacetone were generated with varying CTABr concentrations and a constant concentration of sulfonamide, an example of which may be found in Figure 2.3. The absorbances at λ_{MAX} of approximately 250 nm and 312 nm were recorded, corresponding to the keto and enol forms of benzoylacetone, respectively. The plots of absorbance at these wavelengths versus CTABr concentration show discontinuities, the concentration of which was taken as the C_{CMC} of CTABr[24].

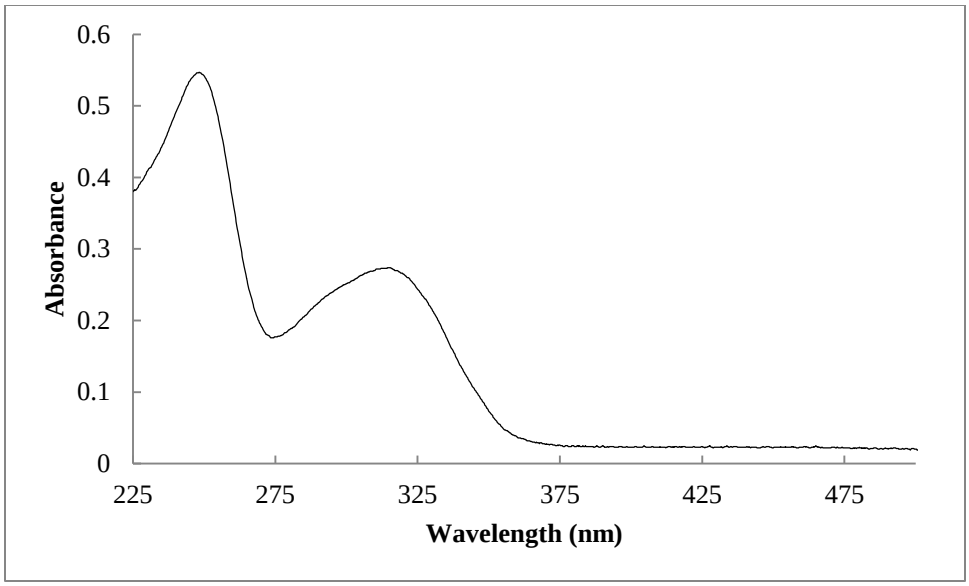

Figure 2.3 UV-Vis Absorbance Spectrum of Benzoylacetone and CTABr

Solutions were analyzed in ascending concentration of CTABr to ensure that minimum cross-contamination occurred, and were cleaned with water, methanol, and dichloromethane following use, followed with drying under nitrogen.

2.3 Results & Discussion

2.3.1 C_{CMC} Determination

Initial NMR studies showed that change in chemical shifts were occurring at concentrations well below the C_{CMC} for CTABr $9x10^{-4}$M in water[24]. As such, studies were undertaken to determine the effect of solvent (H_2O or D_2O) and the presence of sulfonamides at concentrations used in NMR experiments on the value of C_{CMC}.

To determine C_{CMC}, a modification of the method of Dominguez et al. was used, where the keto-enol tautomerization of benzoylacetone was observed via UV-Vis[24]. As the concentration of surfactant increased, the absorbance due to the keto and enol forms changed due to a shift in the tautomerization equilibrium, as can be seen in Figure 2.4.

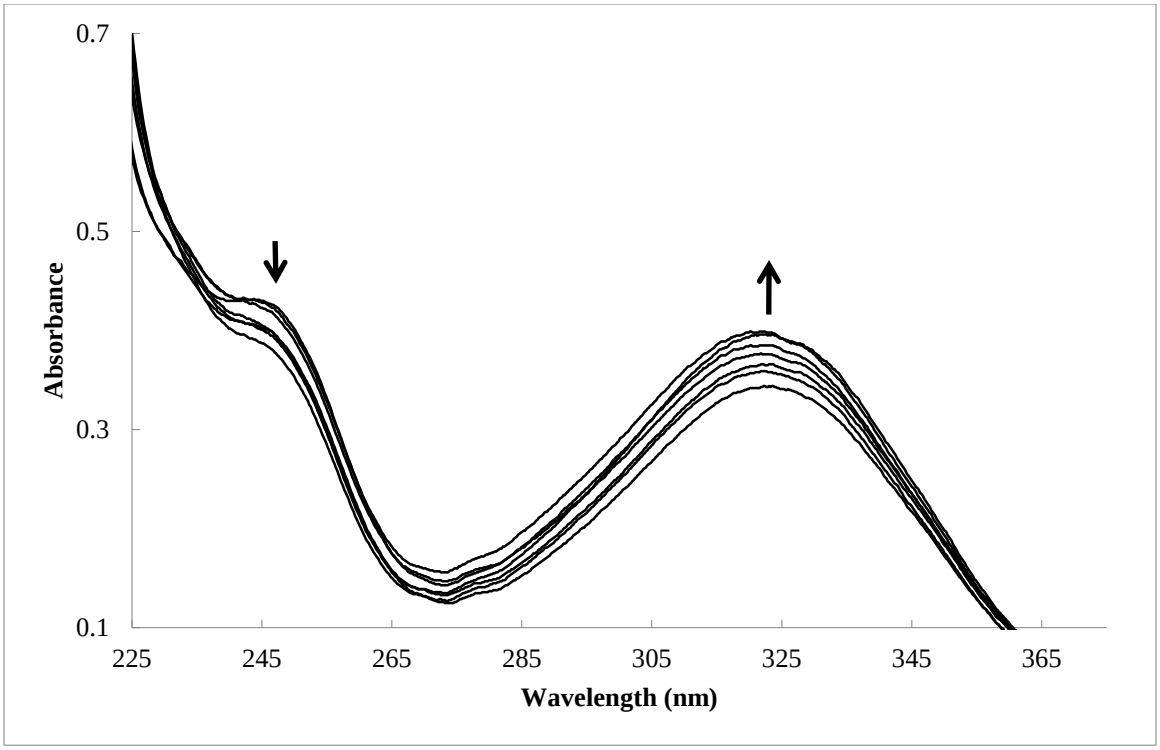

Figure 2.4 Stacked Spectra of BZA in Increasing [CTABr]

When the absorbance at either 250 nm or 312 nm is graphed, a piecewise function corresponding to pre- and post-micellar aggregation is noted, the intersection of which is equal to the C_{CMC}, as seen in Figure 2.5. A small increase in the absorbance at 312 nm is seen prior to reaching C_{CMC} due to sub-micellar inclusion and subsequent shift in the tautomerization equilibrium, however once the C_{CMC} is reached and micelles form, inclusion results in a large shift of the keto-enol tautomerization as shown below.

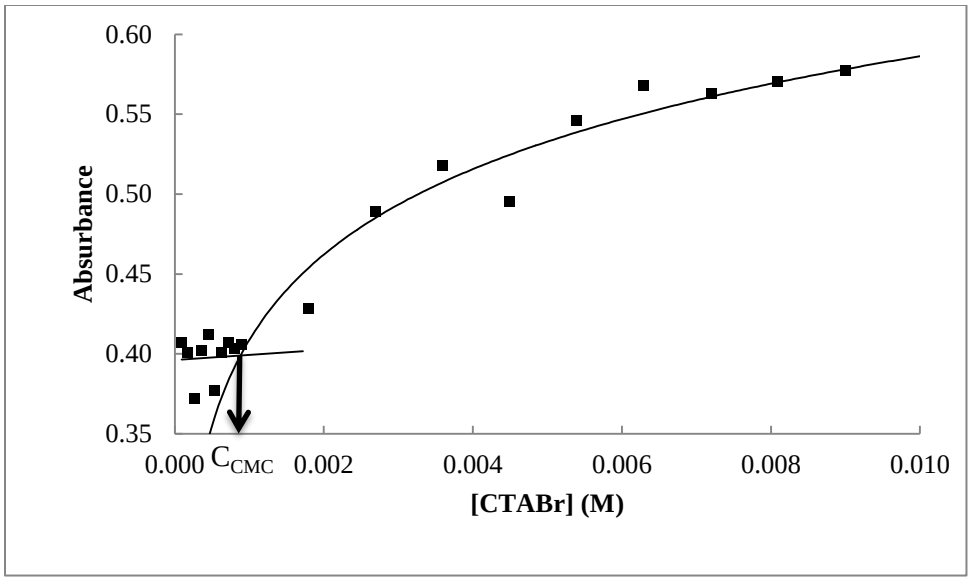

Figure 2.5 Absorbance of BZA at 312 nm with Varying [CTABr]

From graphs such as Figure 2.5, the C_{CMC} values for CTABr under various solvent conditions were calculated, and are tabulated in Table 2.4 below.

Table 2.4 Effect of Solvent and Additive on the C_{CMC} of CTABr

H_2O			D_2O		
Additive	C_{CMC} (M)	Std. Dev. (M)	Additive	C_{CMC} (M)	Std. Dev. (M)
None	8.93×10^{-4}	0.33×10^{-4}	None	6.88×10^{-4}	1.23×10^{-4}
4 (5.04×10^{-4} M)	9.60×10^{-4}	0.65×10^{-4}	4 (5.13×10^{-4} M)	7.24×10^{-4}	1.97×10^{-4}
5 (5.07×10^{-4} M)	1.06×10^{-3}	0.15×10^{-3}	5 (4.87×10^{-4} M)	1.07×10^{-3}	0.28×10^{-3}
7 (4.90×10^{-4} M)	4.65×10^{-4}	2.12×10^{-4}	7 (4.75×10^{-4} M)	3.82×10^{-3}	0.07×10^{-3}
8 (5.12×10^{-4} M)	1.00×10^{-3}	0.12×10^{-3}	8 (5.12×10^{-4} M)	7.01×10^{-4}	1.62×10^{-4}

Clearly, the use of D_2O as a solvent lowers the value of C_{CMC}; however each sulfonamide appears to have a different effect on the C_{CMC}. Thus, in our previous binding constant fitting, it is understandable that each sulfonamide would have a different value for C_{CMC}.

2.3.2 Orientation and Locus

It was desired that by examination of appropriate ^{1}H NMR spectra, the locus and orientation could be determined for sulfonamides, as well as a binding constant (as will be discussed in Section 2.3.3). For each sulfonamide, two graphs were produced, one of a set sulfonamide concentration and varying CTABr concentrations, and one of a set CTABr concentration and a varying sulfonamide concentrations. Relevant conclusions are drawn from the two graphs. Proposed locus and orientations are relevant only when the time-averaged nature of NMR spectra is considered. That is, the measured chemical shift is an average, and so it is possible that multiple orientations within the micelle are possible – the diagram shows only the orientation corresponding to the average location.

NMR studies of the effect of solvent on the chemical shift of a selected probe molecule, sulfamerazine, were also performed and the chemical shifts measured relative to a sealed capillary of D_2O. Unfortunately, attempts to correlate solvent polarity (measured by chemical shift) were unsuccessful, as chemical shifts changed in unpredictable fashions, possibly due to complexation with the solvent.

As the results in Table 2.5 demonstrate, no simple relationship exists and each situation must be considered separate from a definite set of rules regarding chemical shift and solvent polarity.

Table 2.5 Effect of Solvent Polarity on Chemical Shift of Sulfamerazine Protons

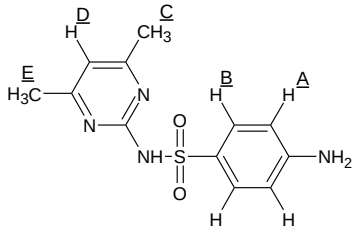

Solvent	Dielectric Constant	Chemical Shift (ppm)				
		A	B	C	D	E
D_2O	78.5	6.75	7.60	7.99	6.61	2.23
DMSO-d_6	46.7	7.30	8.07	8.74	7.00	1.69
Acetonitrile-d_3	37.5	7.59	8.51	9.01	7.41	N/A
Methanol-d_4	32.7	6.71	7.63	8.12	6.53	2.25
Ethanol-d_6	24.5	6.25	7.23	7.69	6.12	1.81

(Note: In Acetonitrile-d3, Proton E was indistinguishable)

2.3.2.1 ^{1}H NMR of Sulfacetamide – Orientation and Locus

Examination of the following plots of ^{1}H chemical shift (δ, ppm) of the sulfonamide non-exchangeable protons with varying CTABr concentration allows for a qualitative determination of the orientation and locus of binding. In Figure 2.7, proton A of sulfacetamide shows a strong upfield shift, consistent with a low polarity environment, while B and C show a slight upfield shift, and thus the entire molecule should be located within the interior of the micelle, with B and C located at roughly the same depth, just beneath the charged layer. This is supported by Figure 2.8, where the chain and terminal methyl CTABr protons show a slight downfield shift from inclusion, and the N-C<u>H</u>$_3$, N-C<u>H</u>$_2$, and N-CH$_2$-C<u>H</u>$_2$ protons show an upfield shift, consistent with a less polar environment caused by inclusion of the sulfonamide. From this, the following qualitative cross-sectional cartoon can be proposed.

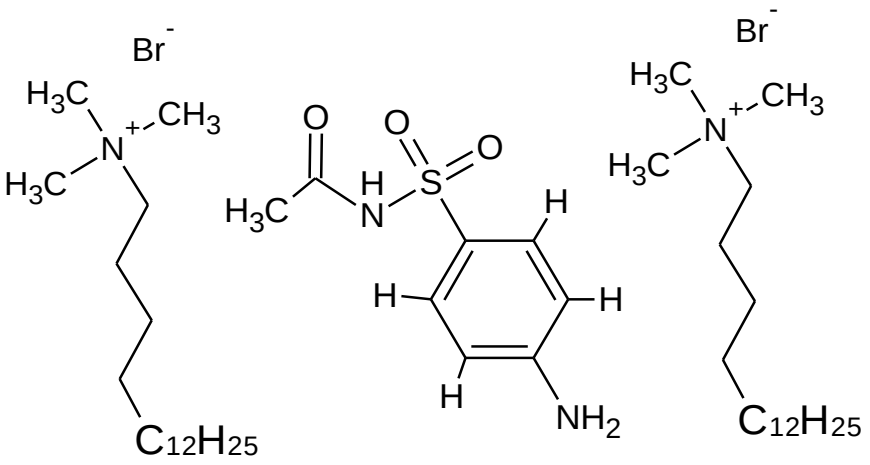

Figure 2.6 Proposed Association of Sulfacetamide with a CTABr Micelle

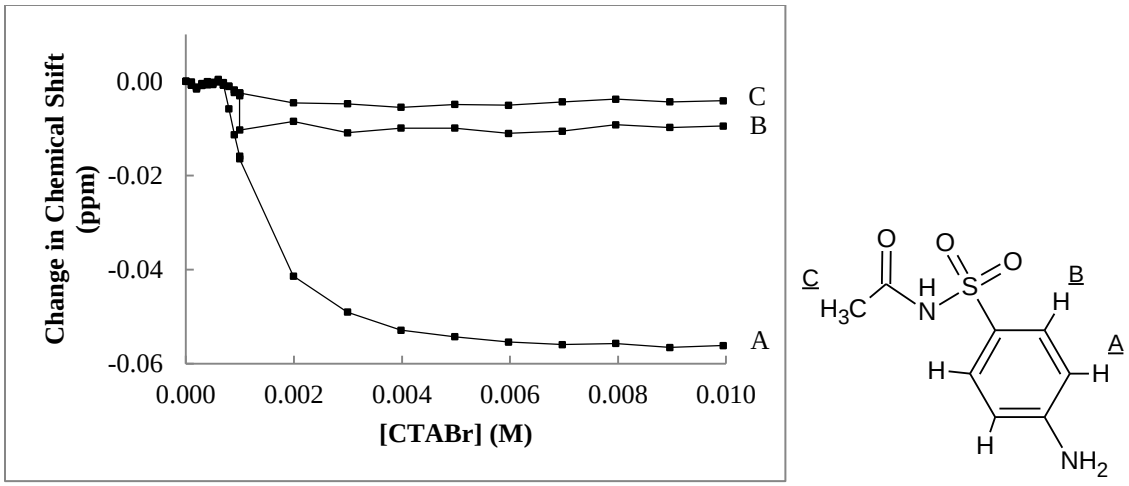

Figure 2.7 Effect of Varying [CTABr] on the ^{1}H NMR Chemical Shifts of Sulfacetamide ([Sulfacetamide] = 2.5x10^{-4} M)

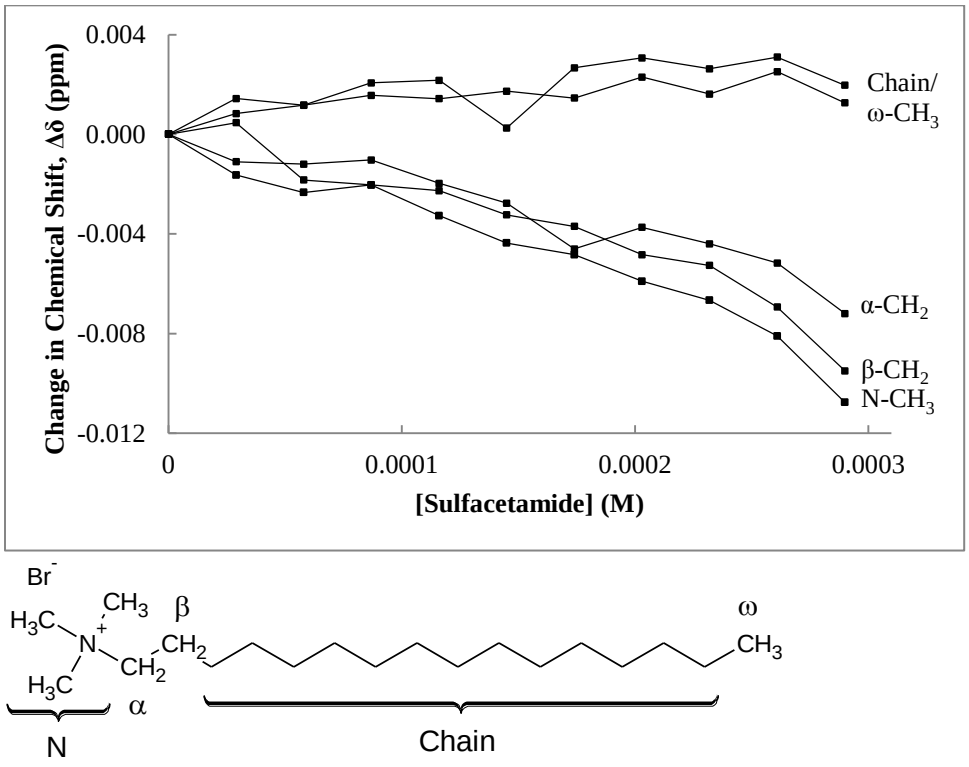

Figure 2.8 Effect of Varying [Sulfacetamide] on the ^{1}H NMR Chemical Shifts of CTABr ([CTABr] = 9.85x10^{-3} M)

2.3.2.2 ^{1}H NMR of Sulfanilamide – Orientation and Locus

Sulfanilamide shows a quite different behavior than sulfacetamide. Unlike sulfacetamide, whose protons showed large shifts post-C_{CMC}, sulfanilamide protons show very little change in chemical shift, either before or after the C_{CMC}. As the concentration of CTABr is increased a very small upfield shift is observed, indicating weak binding, but at higher CTABr concentrations minor inclusion does occur. Thus, the bulk of any association would be purely external to the micelle itself, and if any diagram is to be drawn at all, it should be one which shows a weak surface association, as illustrated in Figure 2.9. At higher concentrations, some slight penetration may occur, but this would be minimal at best.

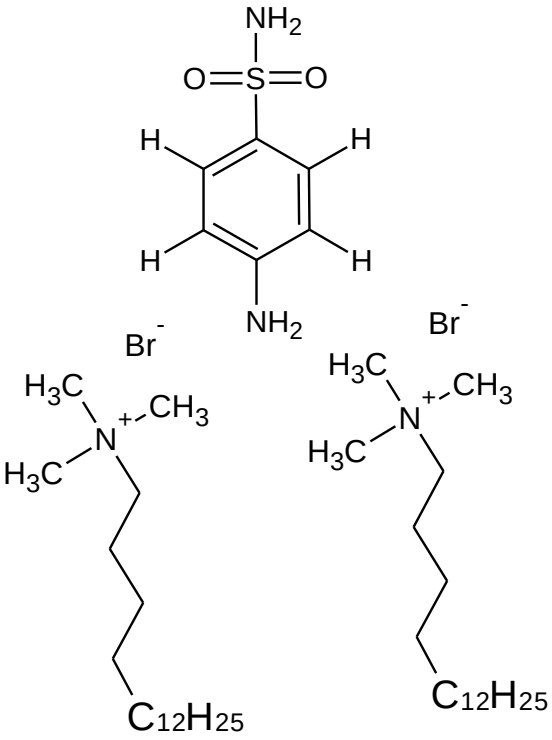

Figure 2.9 Proposed Association of Sulfanilamide with a CTABr Micelle

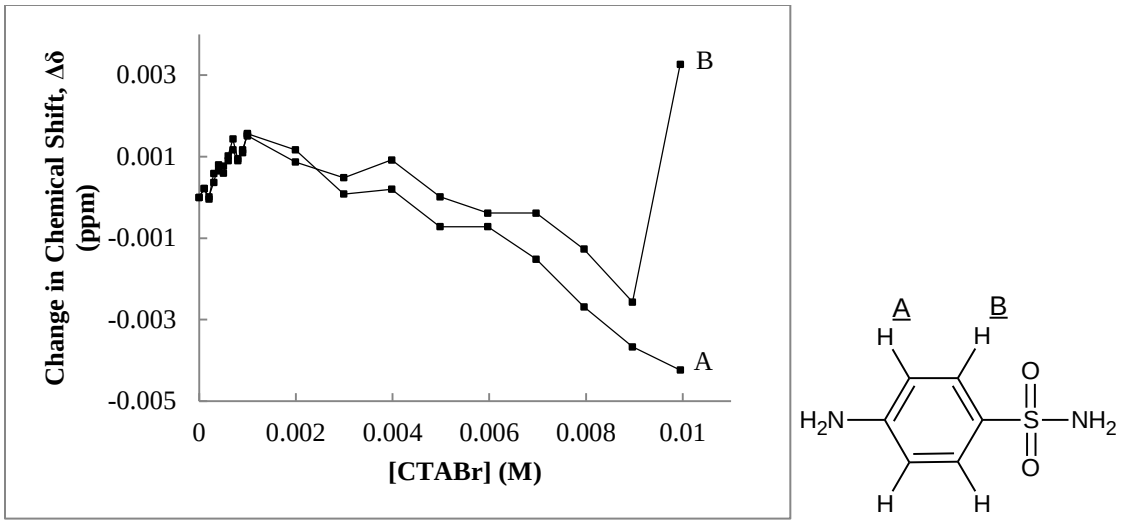

Figure 2.10 Effect of Varying [CTABr] on the ^{1}H NMR Chemical Shifts of Sulfanilamide ([Sulfanilamide] = 2.6x10^{-4} M)

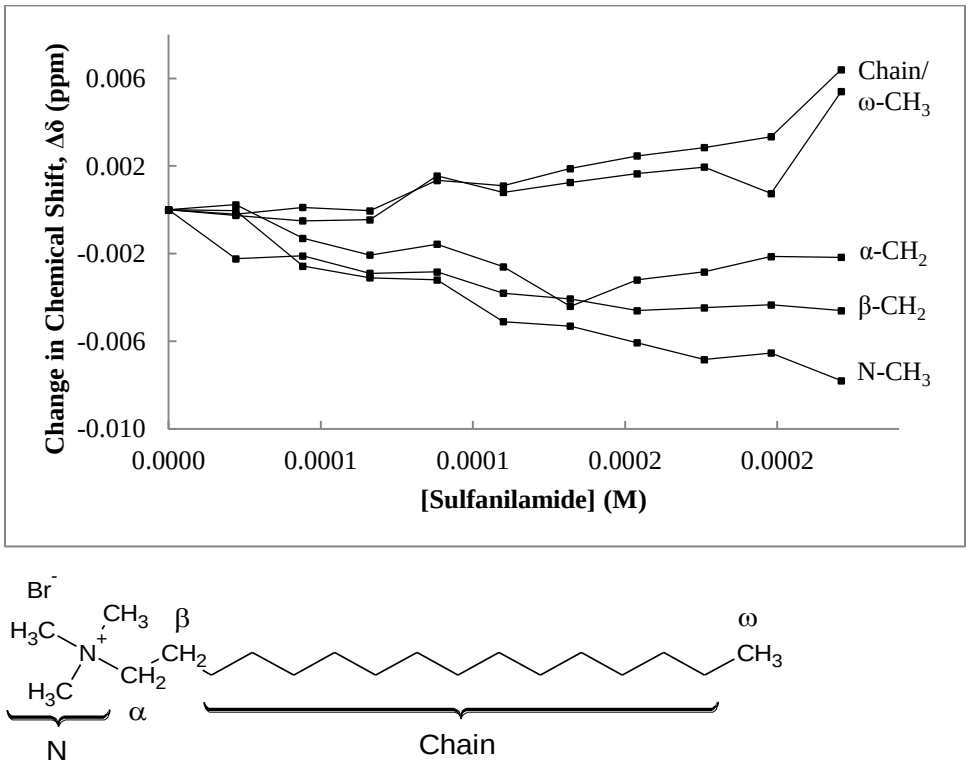

Figure 2.11 Effect of Varying [Sulfanilamide] on the ^{1}H NMR Chemical Shifts of CTABr ([CTABr] = 9.80x10^{-3} M)

2.3.2.3 ^{1}H NMR of Sulfadiazine – Orientation and Locus

Sulfadiazine, bearing a pyrimidine and aniline moiety on either side of the sulfonamide linkage, demonstrates insertion into the hydrophobic core of the micelle, with only the sulfonamide group and the top half of the aniline and pyrimidine rings in the charged layer. Of note is that the hydrogen present in the 3 and 5 positions on both rings show almost exactly the same change in chemical shift behavior, indicating a very similar environment, despite the differences in the aromatic ring on which they are located. This would seem to indicate that the sulfonamide group is the most hydrophilic portion of the molecule, and that it shows the greatest attraction for the positively charged trimethylammonium headgroups, possibly due to a cation-dipole interaction. The aromatic rings then penetrate into the hydrophobic core, stabilized by hydrophobic effects and cation-pi interactions with the headgroups.

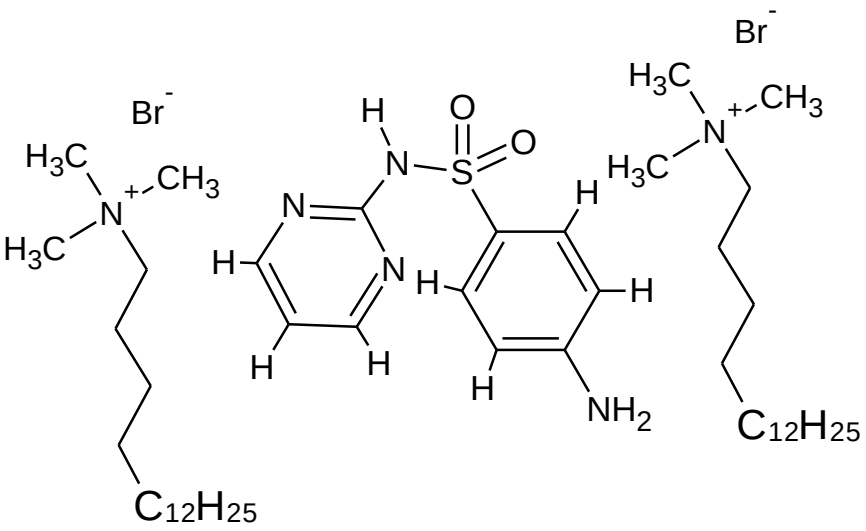

Figure 2.12 Proposed Association of Sulfadiazine with a CTABr Micelle

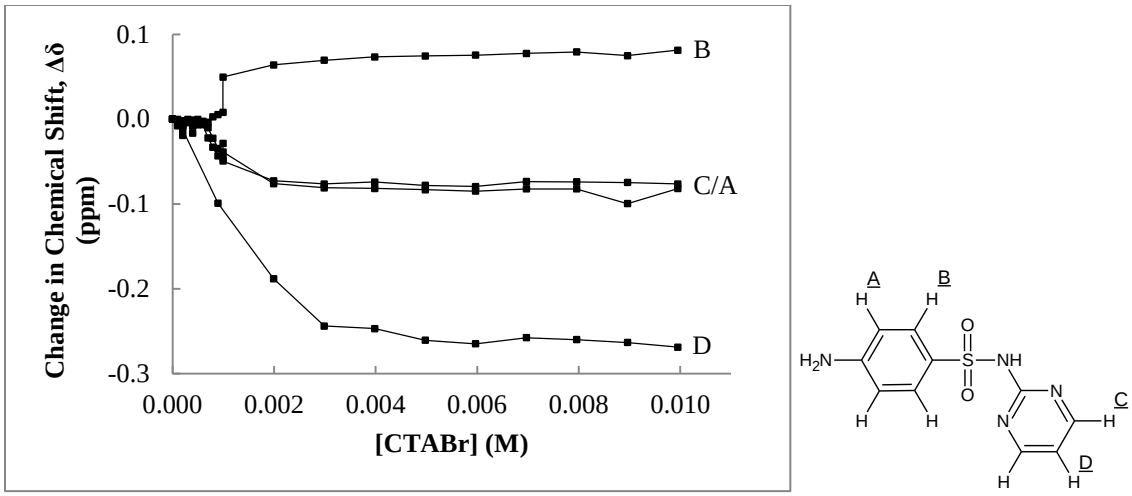

Figure 2.13 Effect of Varying [CTABr] on the ^{1}H NMR Chemical Shifts of Sulfadiazine ([Sulfadiazine] = 2.6x10^{-4} M)

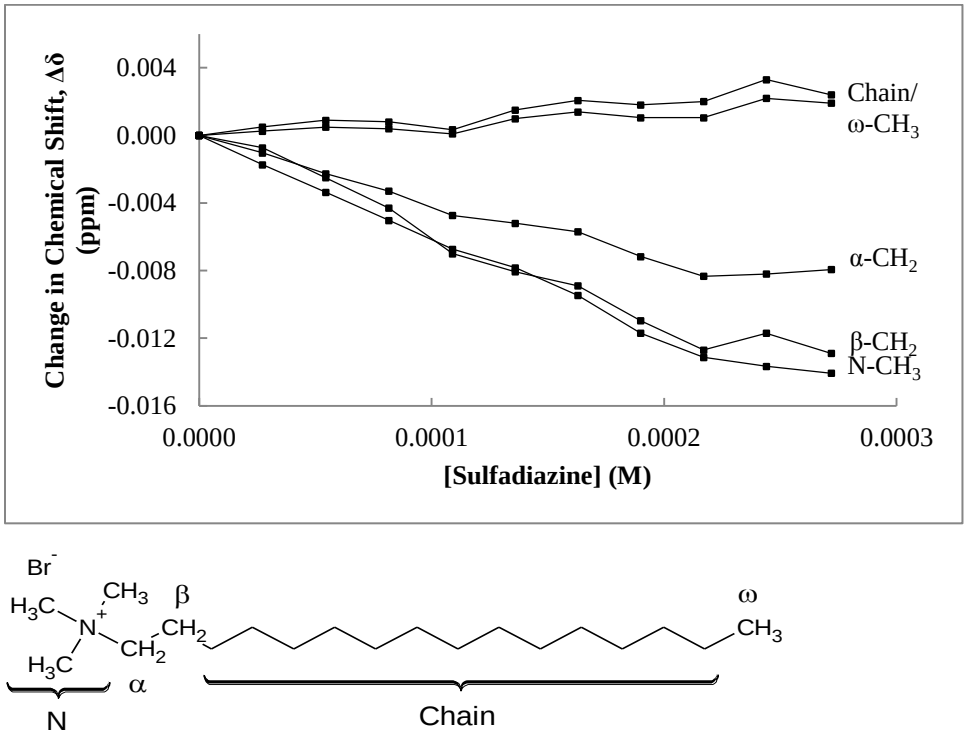

Figure 2.14 Effect of Varying [Sulfadiazine] on the ^{1}H NMR Chemical Shifts of CTABr ([CTABr] = 9.95x10^{-3} M)

2.3.2.4 ^{1}H NMR of Sulfaguanidine – Orientation and Locus

Sulfaguanidine is a close analog to sulfacetamide where the terminal acetyl has been functionalized into a guanidine. The most obvious effect would be the lowering of the pK_b (guanidine itself has a pK_b = 1.5). Thus, in solution, it would be expected that this molecule can be easily protonated., as indicated below. This would first have the effect of imparting the molecule with a positive charge at one end; however in the process it would separate this charge away from the aniline. Thus, a weak binding is observed. Figure 2.17 describes the data – the downfield shift experienced by the $NC\underline{H}_3$, $NC\underline{H}_2$, and $NCH_2C\underline{H}_2$ is consistent with these hydrogen being brought into a closer proximity with a positive charge. Thus, the following diagram can be suggested, where the sulfonamide partitions to the charged layer and at higher concentrations is forced deeper into the micelle.

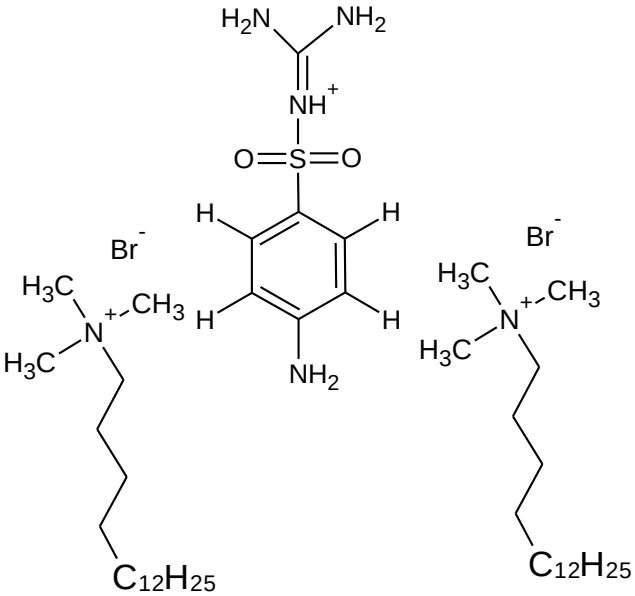

Figure 2.15 Proposed Association of Sulfaguanidine with a CTABr Micelle

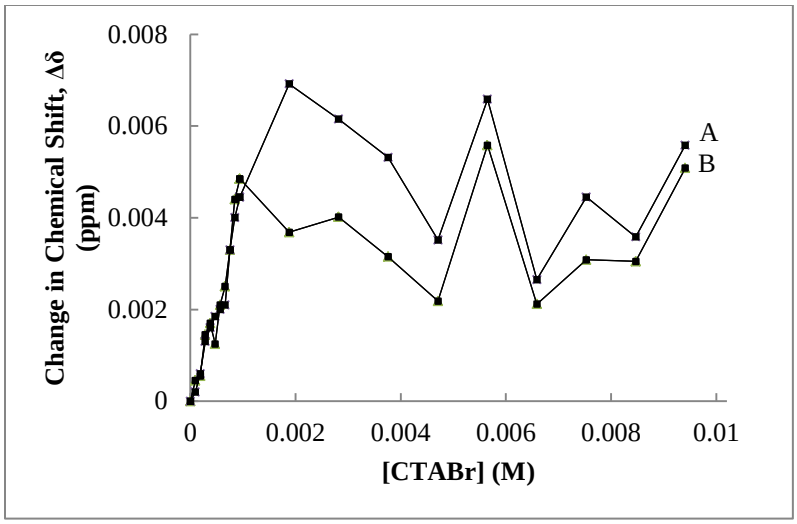

Figure 2.16 Effect of Varying [CTABr] on the ^{1}H NMR Chemical Shifts of Sulfaguanidine ([Sulfaguanidine] = 3.4x10^{-4} M)

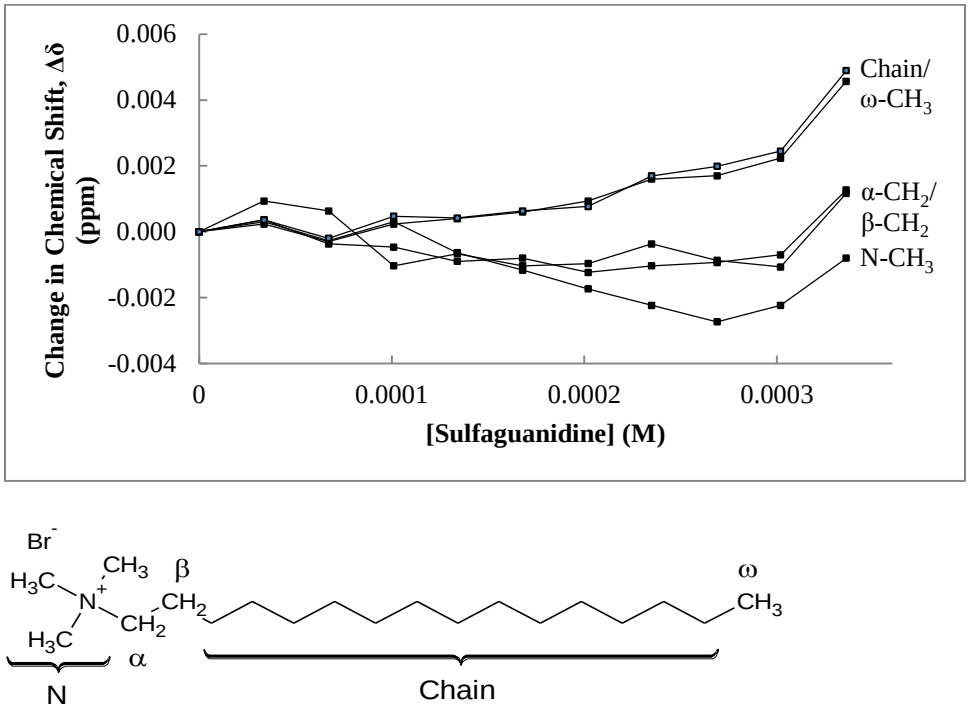

Figure 2.17 Effect of Varying [Sulfaguanidine] on the ^{1}H NMR Chemical Shifts of CTABr ([CTABr] = 8.96x10^{-3} M)

2.3.2.5 ^{1}H NMR of Sulfamerazine – Orientation and Locus

The behavior of sulfamerazine shows some similarities to previous sulfonamides with an aromatic ring on each side of the sulfonamide group. The high downfield shift of B combined with the high upfield shift of A would seem to indicate that the aniline ring is located close to the charged layer, while the pyridinium ring is located more internally, possibly due to the hydrophobic nature of the methyl group. Interestingly, the methyl does not show behavior indicative of inclusion. If there is in fact a cation-pi binding occurring, then aromatic protons will be affected more than methyl protons, as their environment is being affected much more by distance from the cation, having direct effects on the local electronic field.

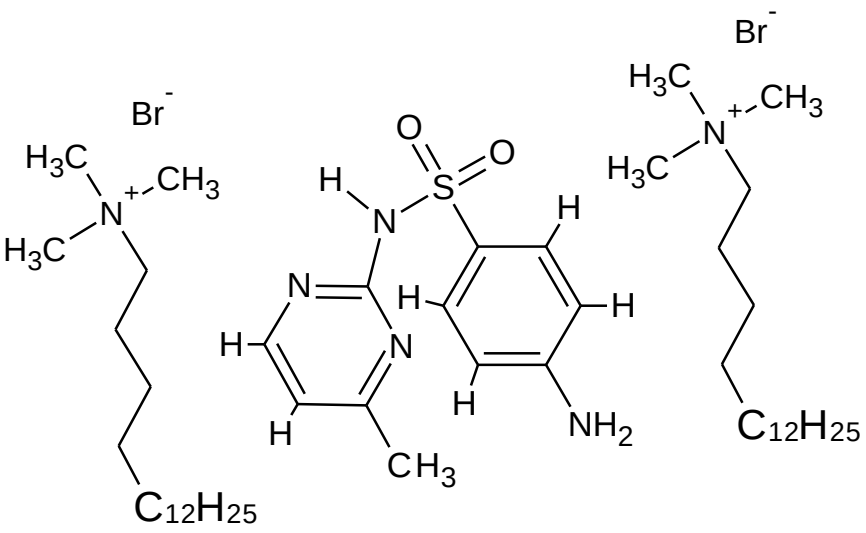

Figure 2.18 Proposed Association of Sulfamerazine with a CTABr Micelle

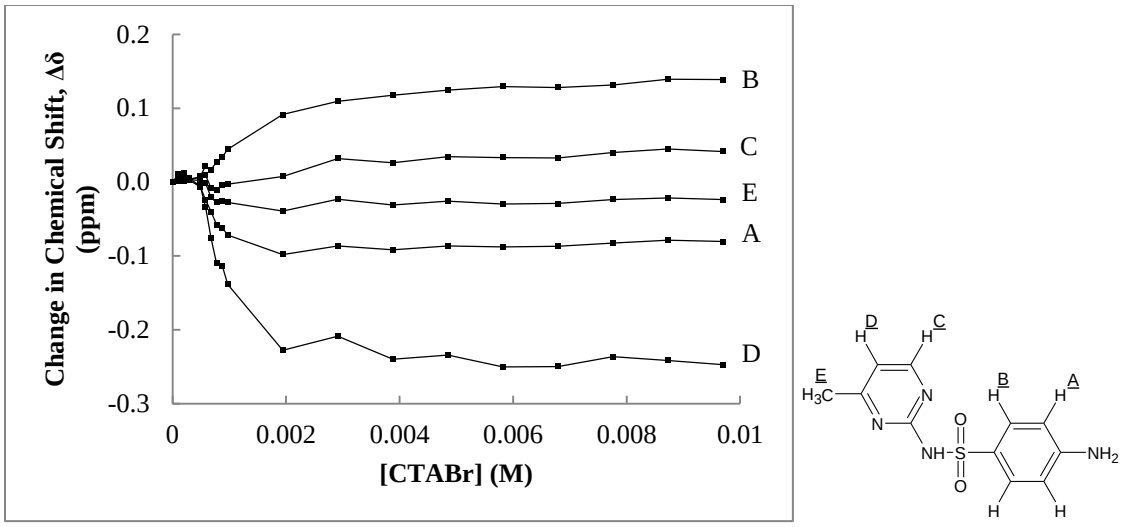

Figure 2.19 Effect of Varying [CTABr] on the ^{1}H NMR Chemical Shifts of Sulfamerazine ([Sulfamerazine] = 3.8x10^{-4} M)

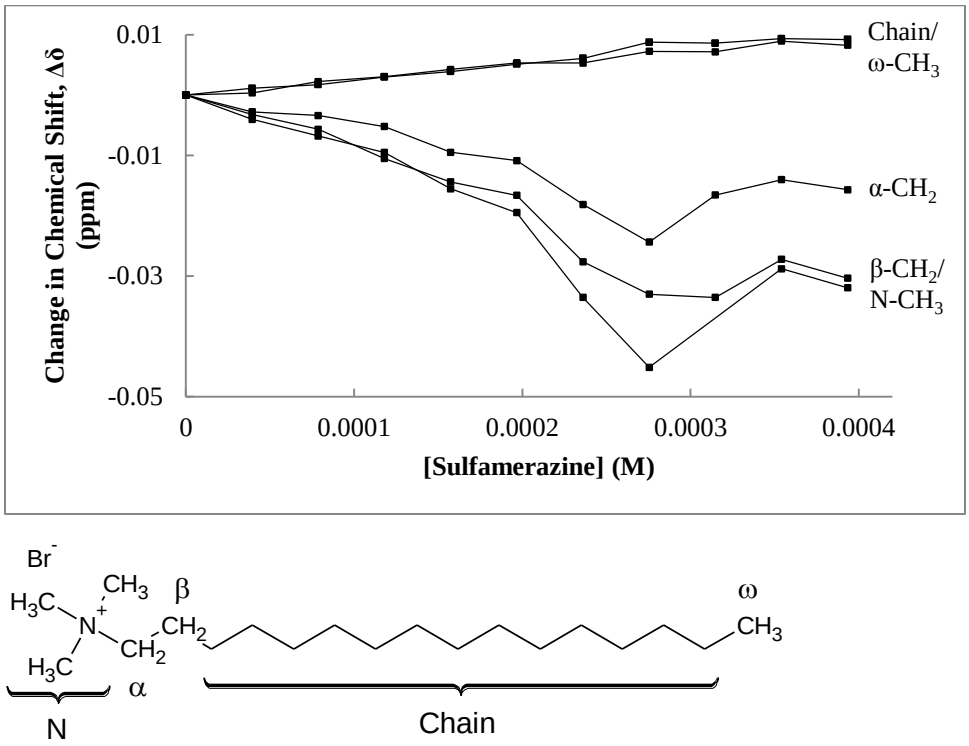

Figure 2.20 Effect of Varying [Sulfamerazine] on the ^{1}H NMR Chemical Shifts of CTABr ([CTABr] = 8.96x10^{-3} M)

2.3.2.6 ^{1}H NMR of Sulfamethoxazole – Orientation and Locus

Sulfamethoxazole shows behavior that is somewhat similar to previous sulfonamides, but presents some interesting challenges. The A and B protons on the aniline show a slight upfield shift, indicating that they are located within the less polar region of the micelle. This is as expected from previous sulfonamide analogs. The methoxazole ring however poses some issues. Unlike sulfamerazine, where the methyl on the aromatic ring showed very little change in chemical shift, here a strong upfield shift is seen. This would indicate that the methyl is somehow located within the hydrophobic region, but that it experiences this more strongly than the methyl on sulfamerazine. The lone proton directly connected to the sulfamethoxazole shows an extremely strong downfield shift, approximately 0.2 ppm. This would indicate that it is directly within the charged layer. This behavior is contradictory to what we would expect, note however that as the structures proposed are merely weighted averages of the true association complexes, two or more forms likely exist.

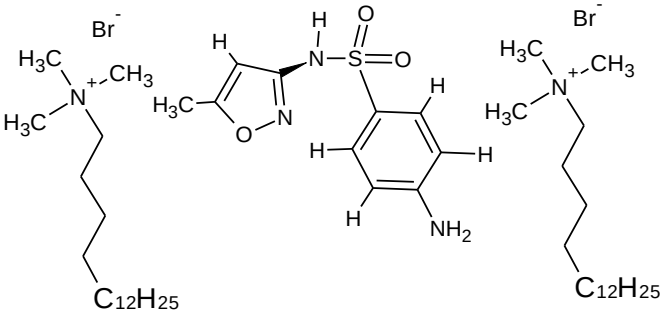

Figure 2.21 Proposed Association of Sulfamethoxazole with a CTABr Micelle

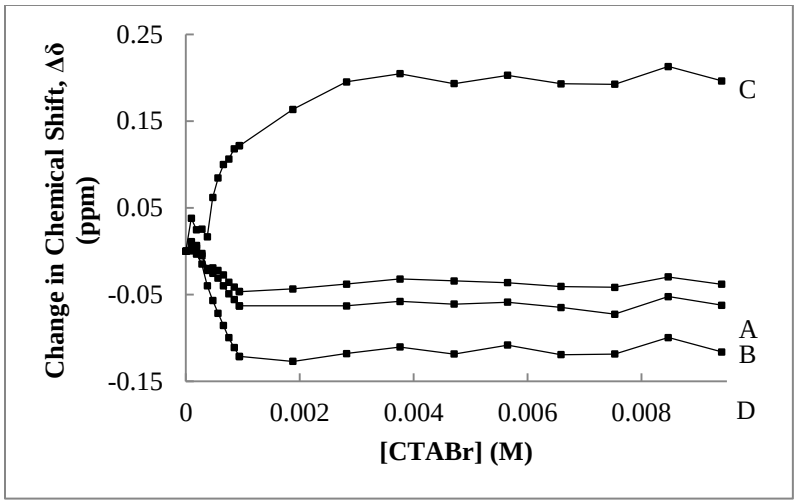

Figure 2.22 Effect of Varying [CTABr] on the ^{1}H NMR Chemical Shifts of Sulfamethoxazole ([Sulfamethoxazole] = 4.8x10^{-4} M)

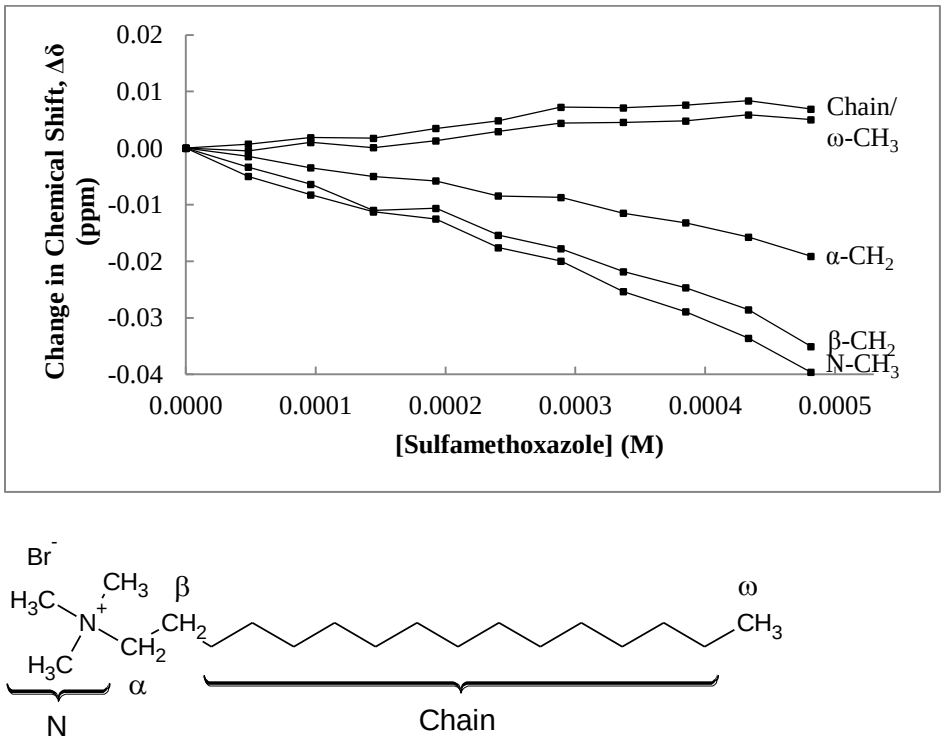

Figure 2.23 Effect of Varying [Sulfamethoxazole] on the ^{1}H NMR Chemical Shifts of CTABr ([CTABr] = 8.96x10^{-3} M)

2.3.2.7 ^{1}H NMR of Sulfathiazole – Orientation and Locus

Sulfathiazole shows relatively straightforward behavior. The aniline ring behaves as expected, with the A protons showing a much stronger upfield shift than the B protons, which show very little shift. The C proton of thiazole is shifted further upfield than the D proton, indicating deeper penetration. Thus, the nitrogen of thiazole must coordinate more strongly with the trimethylammonium headgroup than the sulfur, resulting in D being in closer proximity to the charged layer than C. Indeed, D and B are in almost the same environment as shown by their very similar change in chemical shift, allowing Figure 2.24 to be proposed.

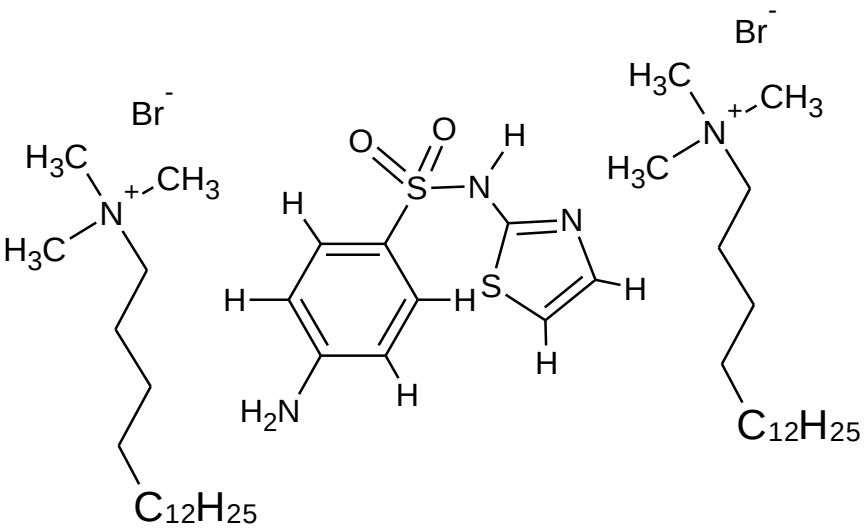

Figure 2.24 Proposed Association of Sulfathiazole with a CTABr Micelle

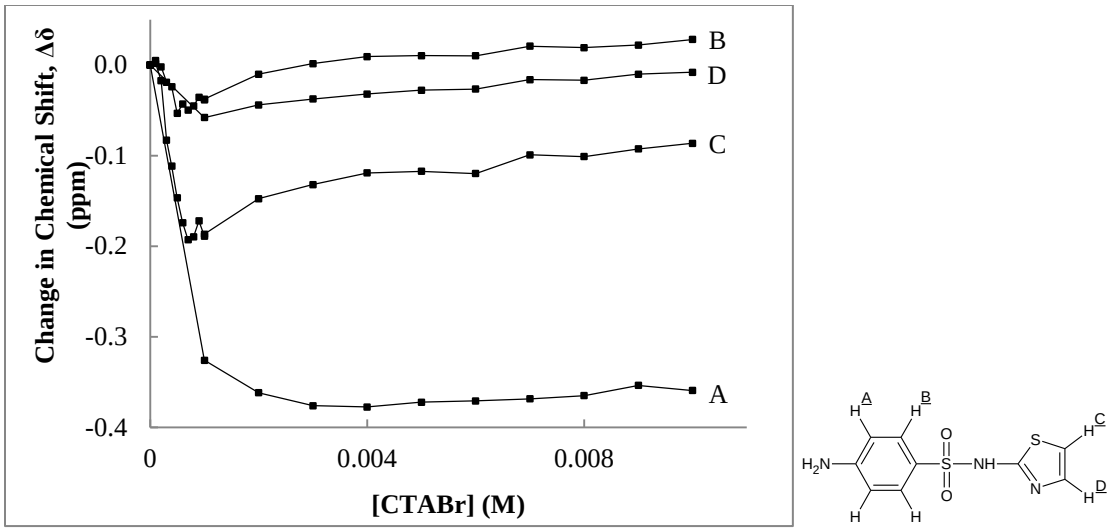

Figure 2.25 Effect of Varying [CTABr] on the ^{1}H NMR Chemical Shifts of Sulfathiazole ([Sulfathiazole] = 4.1x10^{-4} M)

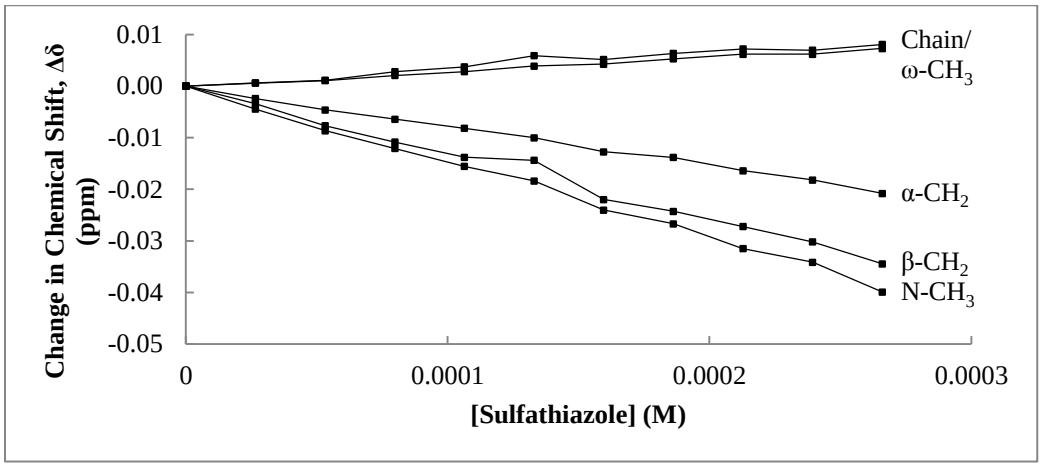

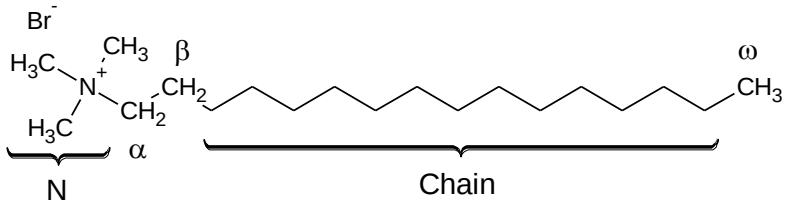

Figure 2.26 Effect of Varying [Sulfathiazole] on the ^{1}H NMR Chemical Shifts of CTABr ([CTABr] = 8.96x10^{-3} M)

2.3.3 Binding Constants

In addition to the orientation and locus of binding, it is possible to fit change in chemical shift to a binding curve so as to generate a binding constant. In all cases, it is the chemical shift of the sulfonamide linkage proton with changing CTABr concentrations which is fit. This equation has been shown previously, and is labeled as Equation 2.2.

To perform fitting, a minimum change in chemical shift of 0.01 ppm was required for a proton, as the error in chemical shift is taken to be 0.001 ppm. For this reason, sulfanilamide and sulfaguanidine were not fit, and no binding constants generated for these analogs. In cases where an analog had at least one proton with a change in chemical shift above 0.01 ppm, all protons were fit regardless of their change in chemical shift.

Sulfamethazine was examined by NMR but the spectra could not be interpreted due to low concentrations and overlapping peaks.

Locus data suggest that each of the following compounds should exhibit measurable binding constants, and that all protons are located in either the charged layer or micellar interior. Therefore, application of Equation 2.2 to fit the data should yield useable binding constants.

Of note in the subsequent analyses was that the value for K_B varies between non-equivalent protons. This is interesting, as binding constant is taken to be a bulk property of a molecule. This phenomenon however has been shown previously in the literature, and was reported as early as 1969 by Foreman et

al.[25] It is also possible that this is an artifact of the fitting process, as the estimated values for C_{CMC} vary between individual protons as well, and in certain cases are associated with an extraneous binding constant.

The results of the subsequent analysis is tabulated below in Table 2.6.

Table 2.6 Binding Constants for Sulfonamides as Determined by ^{1}H NMR

Compound	log(K_B) Range	Average log(K_B)
Sulfacetamide	3.57-3.97	3.84+/- 0.21
Sulfadiazine	3.58-4.05	3.81 +/- 0.20
Sulfamerazine	2.87-4.56	4.11 +/- 0.67
Sulfamethoxazole	3.43-4.65	4.35 +/- 0.53
Sulfathiazole	2.57-3.40	3.12 +/- 0.40

2.3.3.1 ^{1}H NMR of Sulfacetamide – Binding Constant

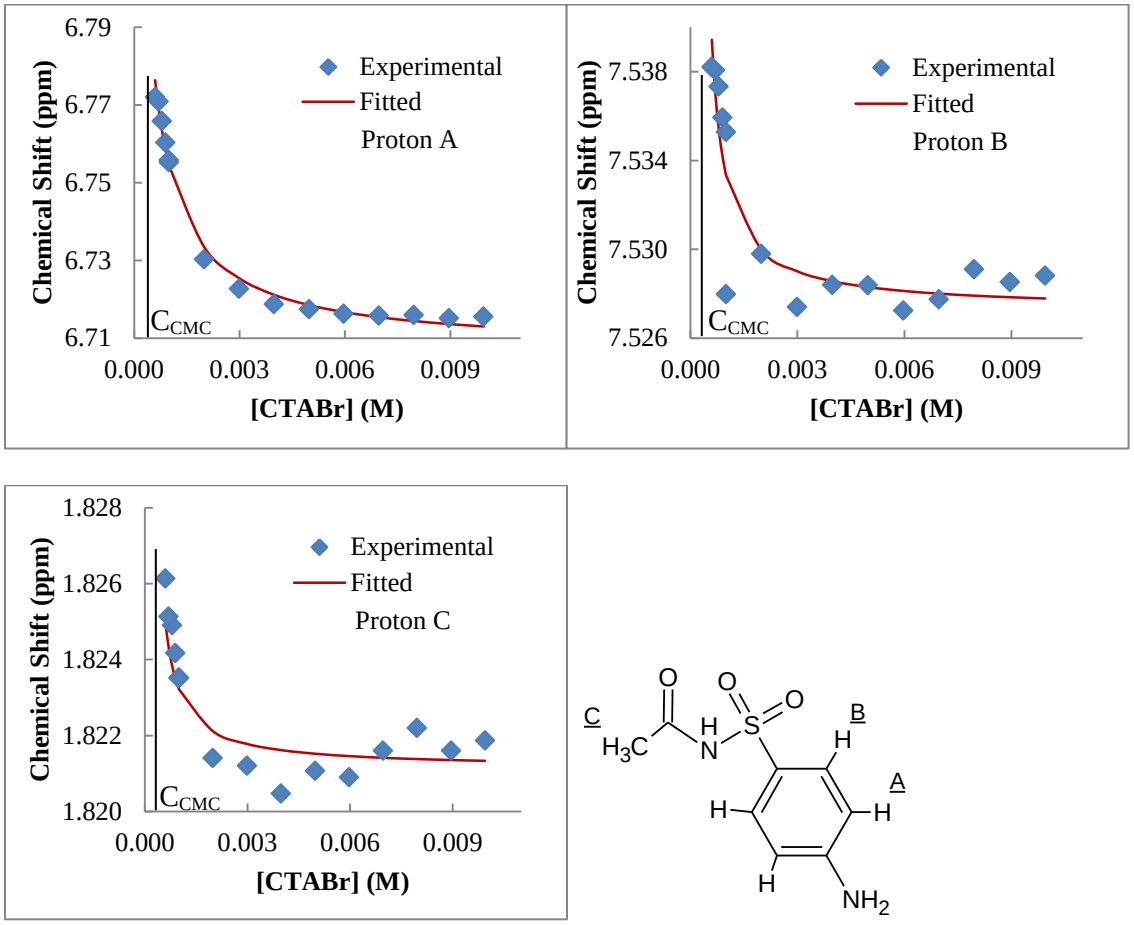

Figure 2.27 Binding Curves for Sulfacetamide

Table 2.7 Binding Fit Parameters for Sulfacetamide

Proton	δ_0 (ppm)	δ_M (ppm)	M (L/mol)	C_{CMC} (M)	$\Sigma(\text{Residuals})^2$	$\log(K_B)$
A	6.772	6.707	$1.09\text{x}10^{3}$	$6.60\text{x}10^{-4}$	$7.04\text{x}10^{-5}$	3.57
B	7.538	7.527	$2.30\text{x}10^{3}$	$6.37\text{x}10^{-4}$	$4.84\text{x}10^{-5}$	3.89
C	1.826	1.821	$2.77\text{x}10^{3}$	$4.88\text{x}10^{-4}$	$7.49\text{x}10^{-6}$	3.97

2.3.3.2 ^{1}H NMR of Sulfadiazine – Binding Constant

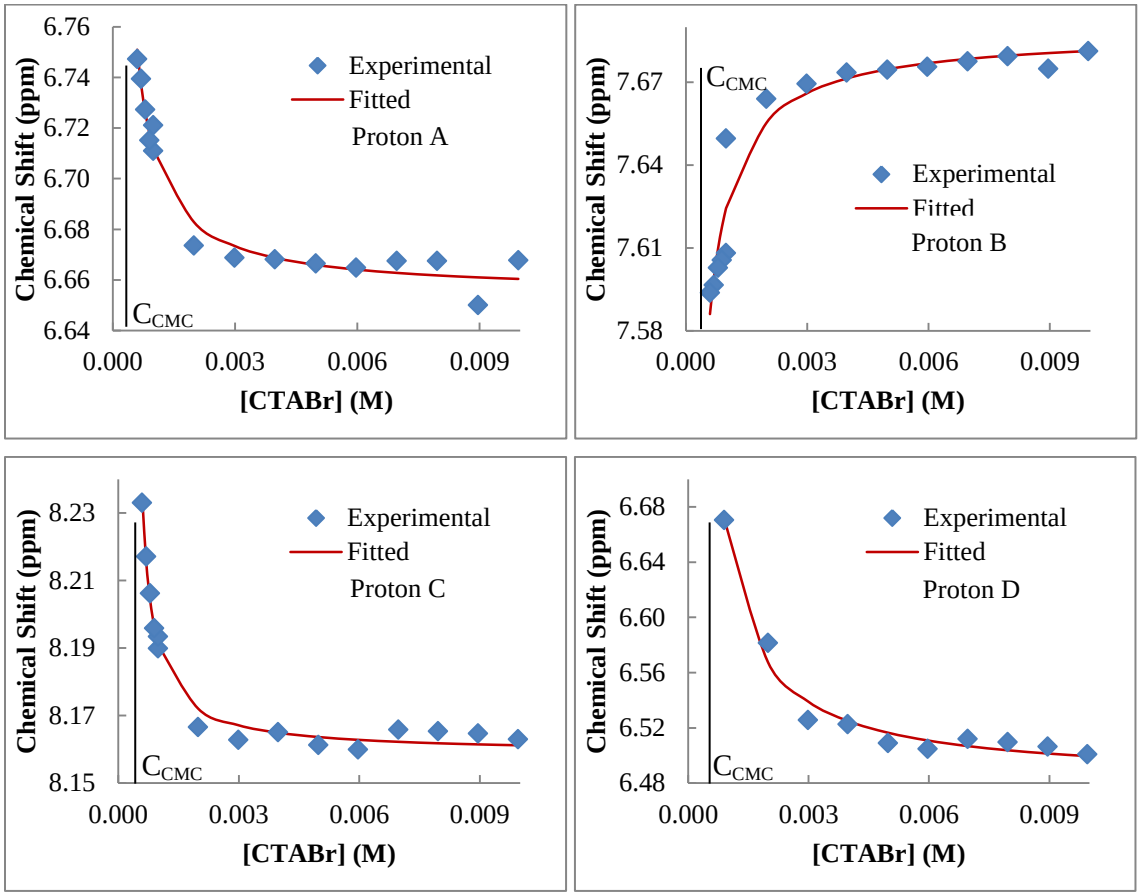

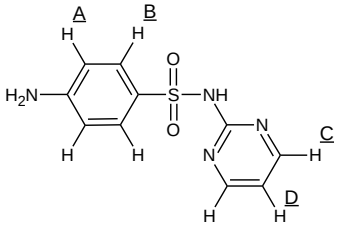

Figure 2.28 Binding Curves for Sulfadiazine

Table 2.8 Binding Fit Parameters for Sulfadiazine

Proton	δ_0 (ppm)	δ_M (ppm)	M (L/mol)	C_{CMC} (M)	$\Sigma(\text{Residuals})^2$	$\log(K_B)$
A	6.747	6.655	1.68×10^{3}	6.20×10^{-4}	4.60×10^{-4}	3.76
B	7.594	7.688	1.40×10^{3}	6.50×10^{-4}	1.29×10^{-3}	3.68
C	8.233	8.159	3.35×10^{3}	6.03×10^{-4}	1.19×10^{-4}	4.05
D	6.670	6.483	1.11×10^{3}	9.02×10^{-4}	5.69×10^{-4}	3.58

2.3.3.3 ^{1}H NMR of Sulfamerazine – Binding Constant

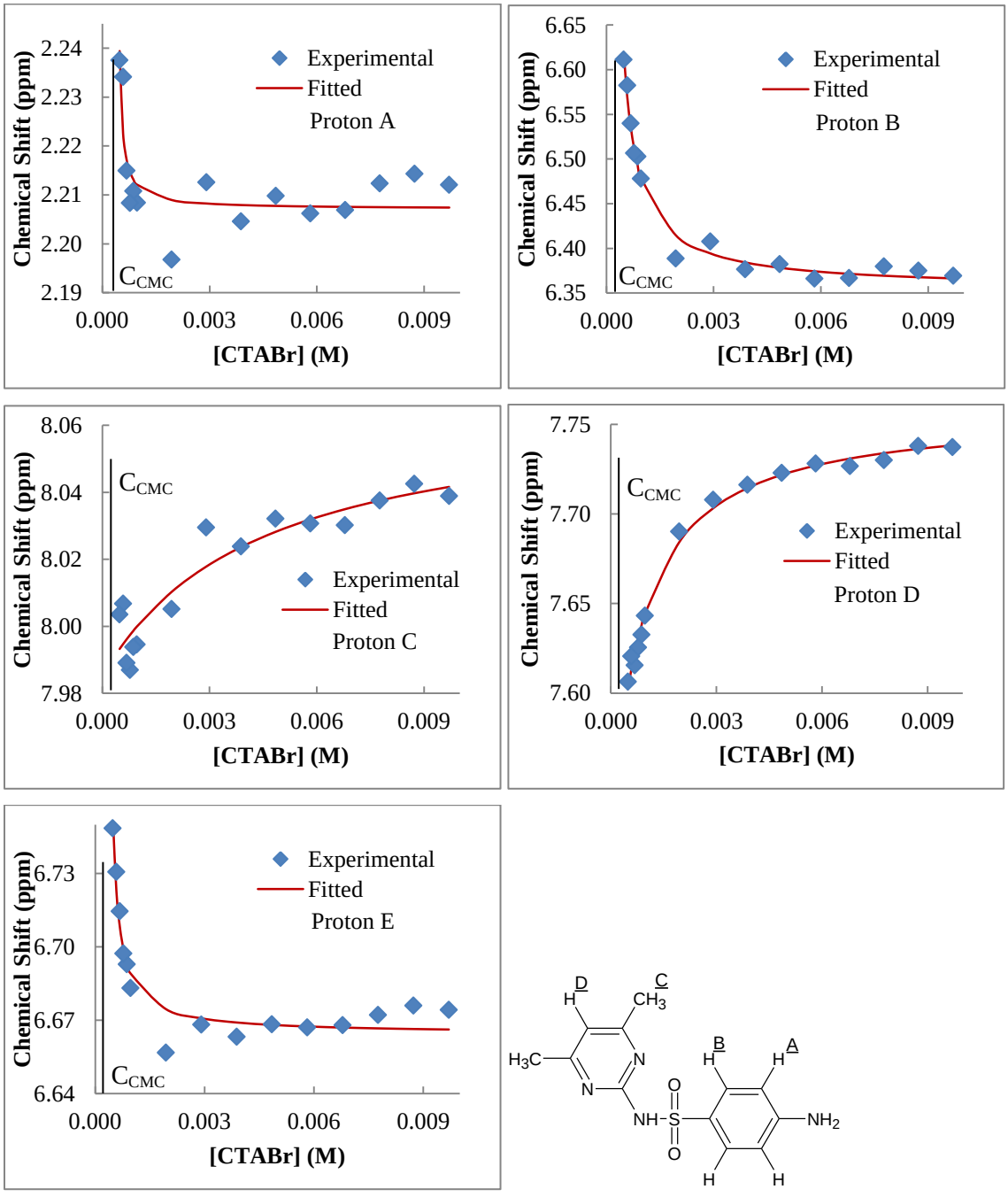

Figure 2.29 Binding Curves for Sulfamerazine

Table 2.9 Binding Fit Parameters for Sulfamerazine

Proton	δ_0 (ppm)	δ_M (ppm)	M (L/mol)	C_{CMC} (M)	$\Sigma(\text{Residuals})^2$	$\log(K_B)$
A	2.238	2.207	1.06×10^{4}	4.90×10^{-4}	4.79×10^{-4}	4.56
B	6.611	6.355	2.27×10^{3}	4.99×10^{-4}	1.54×10^{-3}	3.89
C	7.989	8.067	2.17×10^{2}	2.29×10^{-4}	6.79×10^{-4}	2.87
D	7.606	7.757	7.47×10^{2}	5.20×10^{-4}	2.76×10^{-4}	3.40
E	6.749	6.664	5.06×10^{3}	4.94×10^{-4}	7.09×10^{-4}	4.24

2.3.3.4 ^{1}H NMR of Sulfamethoxazole – Binding Constant

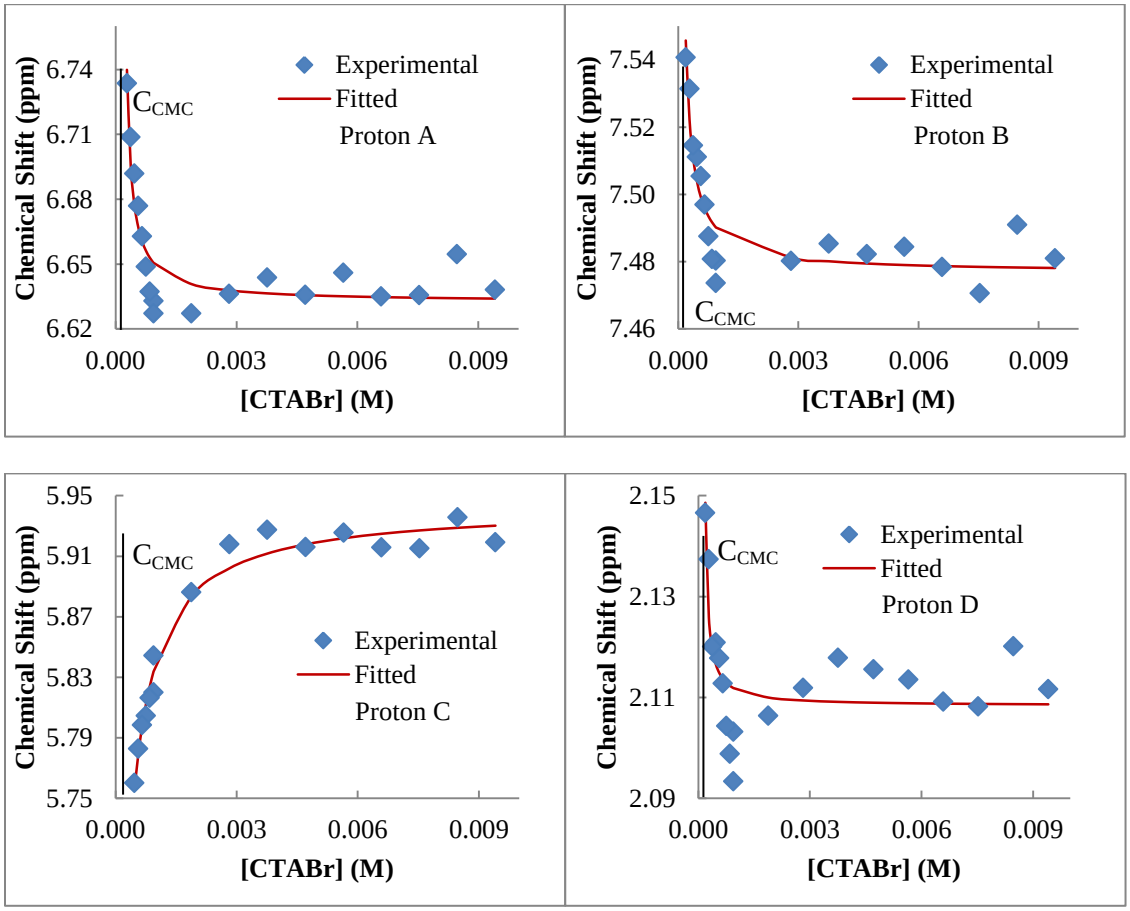

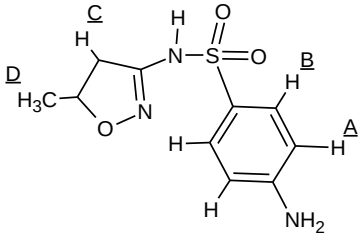

Figure 2.30 Binding Curves for Sulfamethoxazole

Table 2.10 Binding Fit Parameters for Sulfamethoxazole

Proton	δ_0 (ppm)	δ_M (ppm)	M (L/mol)	C_{CMC} (M)	$\Sigma(\text{Residuals})^2$	$\log(K_B)$
A	6.734	6.633	7.06×10^{3}	2.90×10^{-4}	2.50×10^{-3}	4.38
B	7.541	7.477	5.12×10^{3}	2.02×10^{-4}	1.04×10^{-3}	4.24
C	5.844	5.943	7.98×10^{2}	1.06×10^{-3}	1.36×10^{-3}	3.43
D	2.147	2.108	1.31×10^{4}	1.92×10^{-4}	1.14×10^{-3}	4.65

2.3.3.5 ^{1}H NMR of Sulfathiazole – Binding Constant

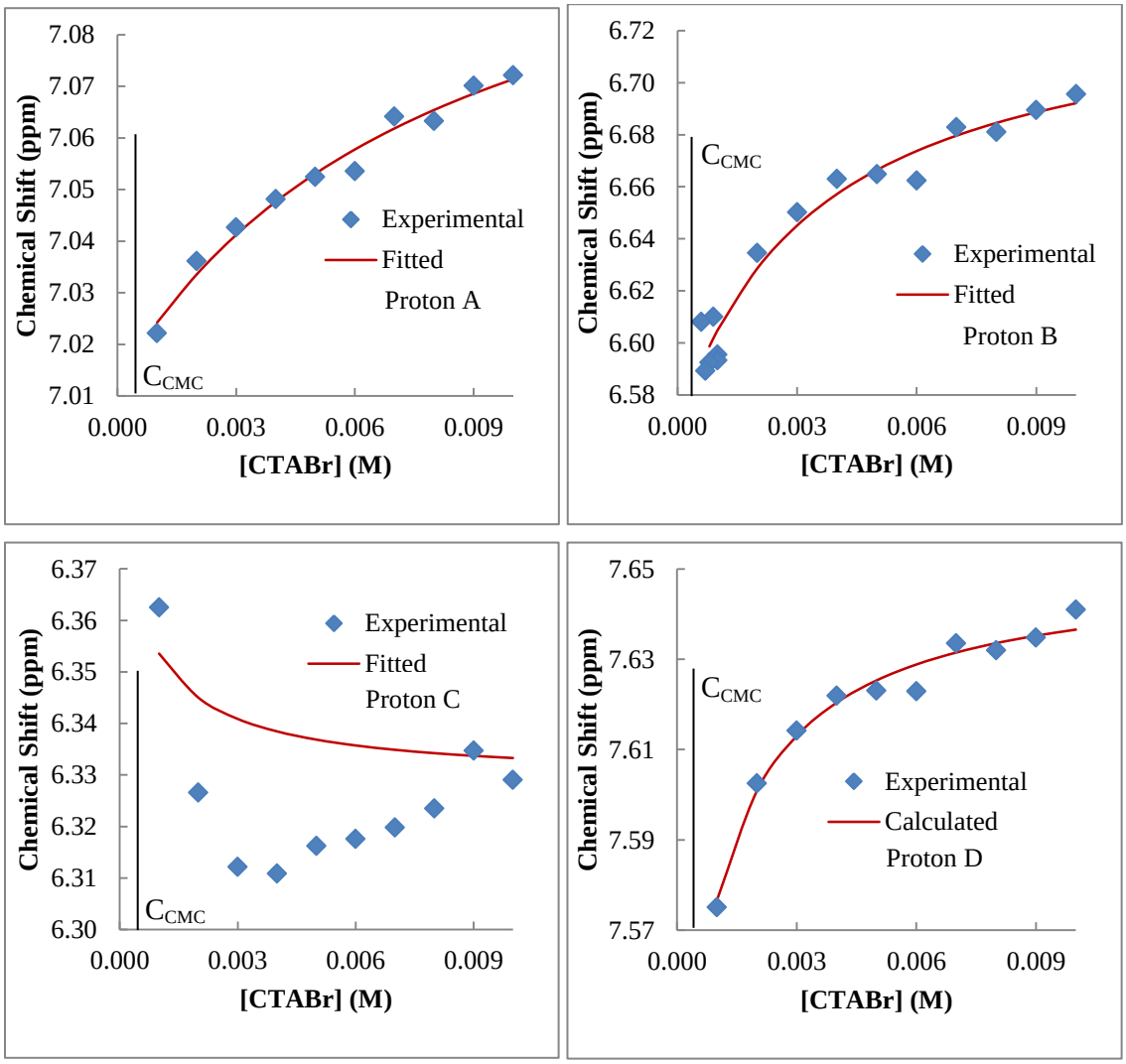

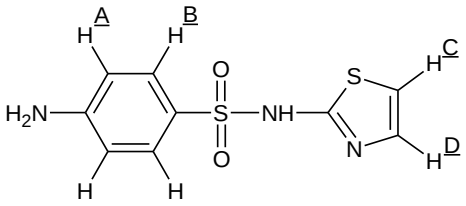

Figure 2.31 Binding Curves for Sulfathiazole

Table 2.11 Binding Fit Parameters for Sulfathiazole

Proton	δ_0 (ppm)	δ_M (ppm)	M (L/mol)	C_{CMC} (M)	$\Sigma(\text{Residuals})^2$	$\log(K_B)$
A	6.363	6.329	7.35×10^{2}	5.00×10^{-4}	3.12×10^{-3}	3.40
B	7.567	7.650	5.51×10^{2}	7.70×10^{-4}	1.01×10^{-4}	3.27
C	6.635	6.736	1.70×10^{2}	2.38×10^{-3}	8.86×10^{-4}	2.76
D	7.022	7.120	1.10×10^{2}	8.07×10^{-4}	4.36×10^{-5}	2.57

2.4 Conclusions

NMR experiments have shown that when association occurs between a sulfonamide and CTABr micelle, the aromatic and ring portions are oriented towards the interior of the micelle with the SO_2NH group nearer to the micelle-water interface. For five analogs (sulfacetamide, sulfadiazine, sulfamerazine, sulfamethoxazole, and sulfathiazole), an orientation and locus within the micelle with associated binding constants has been proposed. For two other analogs, sulfanilamide and sulfaguanidine, low binding is shown by NMR measurements. These two analogs both contain a terminal amino, either at the end of the sulfonamide linkage for sulfanilamide or in the form of a guanidine moiety for sulfaguanidine.

Of issue with the experiments performed is the high concentration of sulfonamide relative to surfactant due to the high concentrations necessary in order to perform NMR spectroscopy. Pseudo-excess conditions are not present in the NMR experiments, and so binding constants may be skewed by overloading of the micelles. As well, the varying values for C_{CMC} demonstrated in Section 2.3.1 indicate that the presence of the sulfonamide is affecting aggregation behavior of the surfactant at the concentrations used for NMR experiments.

It would be desirable to verify NMR results by another method, in particular one which does not have the concentration limitations imposed by the analysis method used previously. Thus, semi-equilibrium dialysis experiments

were performed and quantified by conductivity and liquid chromatography-mass spectrometry, as will be described in the following chapter.

2.5 References

(1) Chaghi, R.; de Menorval, L. C.; Charnay, C.; Derrien, G.; Zajac, J. *J Colloid Interf Sci* **2008**, *326*, 227.

(2) Bernardez, L. A. *Colloid Surface A* **2008**, *324*, 71.

(3) Farias, T.; de Menorval, L. C.; Zajac, J.; Rivera, A. *Colloid Surface A* **2009**, *345*, 51.

(4) Kim, B. J.; Im, S. S.; Oh, S. G. *Langmuir* **2001**, *17*, 565.

(5) Kreke, P. J.; Magid, L. J.; Gee, J. C. *Langmuir* **1996**, *12*, 699.

(6) Magid, L. J.; Han, Z.; Warr, G. G.; Cassidy, M. A.; Butler, P. D.; Hamilton, W. A. *J Phys Chem B* **1997**, *101*, 7919.

(7) Mata, J. P.; Aswal, V. K.; Hassan, P. A.; Bahadur, P. *J Colloid Interf Sci* **2006**, *299*, 910.

(8) Xu, K.; Ren, H. Q.; Zeng, G. M.; Ding, L. L.; Huang, J. H. *Colloid Surface A* **2010**, *356*, 150.

(9) Gao, Z. S.; Wasylishen, R. E.; Kwak, J. C. T. *J Phys Chem* **1989**, *93*, 2190.

(10) Stilbs, P. *J Colloid Interf Sci* **1981**, *80*, 608.

(11) Connors, K. A. *Binding constants : the measurement of molecular complex stability*; Wiley: New York, **1987**.

(12) Fielding, L. *Tetrahedron* **2000**, *56*, 6151.

(13) Carper, W. R.; Buess, C. M.; Hipp, G. R. *J Phys Chem* **1970**, *74*, 4229.

(14) Dust, J. M., Ph.D. Thesis, Queen's University, 1987.

(15) Shirin, S.; Buncel, E.; vanLoon, G. W. *Can. J. Chem.-Rev. Can. Chim.* **2003**, *81*, 45.

(16) Balakrishnan, V. K.; Han, X. M.; Vanloon, G. W.; Dust, J. M.; Toullec, J.; Buncel, E. *Langmuir* **2004**, *20*, 6586.

(17) World Healh Organization, 2010.

(18) Sanli, S.; Altun, Y.; Sanli, N.; Alsancak, G.; Beltran, J. L. *J Chem Eng Data* **2009**, *54*, 3014.

(19) Lin, Y. T.; Liu, Y. W.; Cheng, Y. J.; Huang, H. Y. *Electrophoresis* **2010**, *31*, 2260.

(20) Tappe, W. G.; Zarfl, C.; Kummer, S.; Burauel, P.; Vereecken, H.; Groeneweg, J. *Chemosphere* **2008**, *72*, 836.

(21) Shalaeva, M.; Kenseth, J.; Lombardo, F.; Bastinz, A. *J Pharm Sci* **2008**, *97*, 2581.

(22) Geiser, L.; Henchoz, Y.; Galland, A.; Carrupt, P. A.; Veuthey, J. L. *J Sep Sci* **2005**, *28*, 2374.

(23) US National Library of Medicine.

(24) Dominguez, A.; Fernandez, A.; Gonzalez, N.; Iglesias, E.; Montenegro, L. *J Chem Educ* **1997**, *74*, 1227.

(25) Foreman, M. I.; Foster, R.; Twiselto.Dr *J Chem Soc D - Chem Comm* **1969**, 1318.

Chapter 3

Semi-equilibrium Dialysis and Energy of Transfer Analysis

3.1 Introduction

To characterize a surfactant-sulfonamide system, the use of ^{1}H NMR was described in the previous chapter to determine orientation and locus information, as well as binding constants. For some sulfonamides, the binding constants were relatively consistent between nuclei; however in other cases deviations of greater than an order of magnitude were noted. Thus, a different method for determination of binding constants would be desirable. Early reports of using MEUF for removal of organic contaminants from water sources suggest that semi-equilibrium dialysis (SED) can be used to determine binding constants in order to characterize MEUF[1].

SED is useful as it acts as a small scale model for an ultrafiltration experiment. The basic premise is that if two volumes of water are separated by a membrane with permeability of a set molecular weight, any additives to the water with molecular weight lower than the set value will equilibrate across the membrane in a short period of time (<24 h)[1]. If, however, a surfactant is added at above the C_{CMC} to one side of the membrane, only the monomer will partition across the membrane within a set time period as the micelles are too large. In this manner a concentration polarization can occur for the time period where on one side of the membrane only monomeric surfactant will exist, and on the other

monomer and micelles. Any chemical additive that can partition to a micelle will also show a concentration polarization, and from analysis of surfactant and additive concentrations on each side of the membrane a binding constant can be determined.

Previous literature reports detail the use of SED for analysis of the partitioning of systems such as 4-t-butylphenol in cetylpyridinium chloride[1], various aromatic hydrocarbons in sodium dodecyl benzenesulfonate[2], and more recently arsenic in cetylpyridinium chloride as an analog to MEUF experiments[3]. In each case, the time for cell equilibration was determined experimentally, and was in the range of 16-24 h.

Given the extensive history of SED being used to find binding constants for micellar systems, it should be possible to utilize it for analysis of sulfonamide partitioning. To analyze the permeate and retentate of a SED system, there are multiple possible methods. To quantify the surfactant, conductivity is a common method[4]. Sulfonamide quantification can be performed using methods such as UV-Vis spectroscopy[5] and LC-MS/MS[6].

To determine a binding constant from a SED experiment, the equations required are relatively simple when compared to those required for NMR binding curves. Here, a binding constant is taken to be the ratio of the concentration of sulfonamide in the micellar phase divided by the concentration of sulfonamide in the aqueous phase, as shown by Equation 3.1 below.

$$K_B = \frac{[Sulfonamide]_M}{[Sulfonamide]_A}$$

Equation 3.1 Equation to Determine Binding Constant (K_B) via SED

Where $[Sulfonamide]_M$ = Micellar concentration of the sulfonamide

$$= \frac{(n_{Sulfonamide,Micellar})}{(n_{Surfactant,Micellar} * M_V)}$$

$(n_{Sulfonamide,Micellar})$ = amount of sulfonamide bound to a micellar system;

$(n_{Surfactant,Micellar})$ = amount of surfactant in micellar aggregates; and

M_V = Molar volume of the surfactant.

It is expected that binding constants derived from SED will act as an acceptable surrogate for removal efficiencies for a MEUF system, as many of the principles are similar[1]. With the goal of characterization of micellar systems and application to MEUF, it would be useful to derive a predictive methodology for the determination of binding constants from a series of measured or predicted chemical constants for a molecule, such as K_{OW} or K_a. In this sense, it should be possible to predict binding constants through a free-energy relationship, a correlation between rate constants or equilibrium constants[7]. This type of analysis is detailed in the literature, and has been used to successfully compare K_{OW} and K_B for phenols in anionic micellar systems[8].

In describing micellar systems, we have used empirical equilibrium constants defined as a ratio of concentrations of a sulfonamide in the micellar phase and aqueous phase. Another more fundamental approach to describe an

equilibrium constant uses a thermodynamic treatment based on Gibbs' free energy.

$$\Delta_r G^0 = -RTlnK$$

Equation 3.2 Relation of Standard Gibbs Energy of Reaction to Equilibrium Constant

(Taken from Reference 9)

Where $\Delta_r G^0$ is the change in standard Gibbs energy of a reaction, R is the ideal gas constant, T the temperature, and K the equilibrium constant under consideration.

Using Equation 3.2 it is straightforward to estimate the equilibrium constant for partition into micelles if the change in free energy of a partition process is known. This approach has been successfully reported, with a great deal of the pioneering work performed by Bunton[10] and expanded on by various other groups[11,12] for the partitioning of various substrates to cationic micelles.

It is of interest to determine if there are specific binding interactions occurring between a substrate and micelle. Empirical binding constants do not lend themselves to this type of analysis; however by using free energy calculations it may be possible to elucidate specific binding parameters. For example, it has been computed that the cation-pi binding that occurs between benzene and tetramethylammonium in aqueous solution should be approximately 3 kJ/mol[13]. Micellar partitioning, however, is a combination of not only cation-pi interactions, but also cation-dipole interactions, cation-induced dipole, and

hydrophobic effect interactions, and so exact elucidation of specific processes is complex. However, if the free energy change of partitioning for similar small molecules is examined, it may be possible to determine the contribution of a specific moiety to the partitioning of the entire molecule.

As a basis for comparison, the work of Hirose and Sepulveda[11] gives binding constants for a variety of compounds partitioning with CTABr, a portion of which is tabulated below and which has been converted to change in free energy from association by Equation 3.2.

Table 3.1 Selected Literature Binding Constants for Benzene Derivatives in CTABr [11]

Compound	log(K_B)	ΔG^0
aniline	1.34	-7.7
p-methylaniline	1.64	-9.4
benzoic acid	2.15	-12.2
benzoate anion	3.40	-19.4
phenol	1.83	-10.5
phenoxide anion	3.11	-17.8

Clearly, compounds with anionic character demonstrate higher binding constants. In the case of an oxygen anion, an increase of approximately 7 kJ/mol is seen in the free energy change (the approximate difference between the ΔG^0 for benzoic acid and the benzoate anion and for phenol and the phenoxide anion). Attempts to explain binding constants as measures of free energy must also take into consideration the locus of solubilization, as it has been shown that when various aromatic carboxylic acid derivatives are partitioned to cationic

micelles, the pK_a of very hydrophobic acids can be decreased by 0.5 units, whereas more hydrophilic examples are affected less[14]. This is due to both charge neutralization as well as stabilization of more hydrophobic examples by partitioning to the micellar interior.

Literature reports have suggested that free energy changes can be treated as additive, so that addition of another group in a certain position contributes a set amount to the change in free energy[11,15]. In this manner, it should be possible to explain the change in free energy experienced by a molecule as the sum of individual changes in free energy due to the partitioning of the various parts of the molecule. Using this approach, estimated K_B values could be determined for a variety of molecules simply by examining their structure. This could help guide the development of future MEUF systems.

3.2 Experimental

3.2.1 Materials

Sulfaguanidine, sulfamethoxazole, sulfamerazine, sulfathiazole, sulfamethazine, sulfadoxine, sulfadiazine, sulfacetamide, and sulfanilamide were purchased from Sigma-Aldrich Chemicals (Oakville, Canada) of the highest grade possible and were used without purification. Cetyl trimethylammonium bromide (CTABr) was also purchased from Sigma-Aldrich Chemicals of the highest grade available, and was used without purification.

All solutions were prepared in deionized water, which was obtained by using a Milli-Q system (Millipore, Whitby, ON).

Pierce brand snakeskin dialysis tubing was purchased from Fisher Scientific (Whitby, ON) with a molecular weight cut-off (MWCO) of 7000 Da. Semi-equilibrium dialysis cells were produced in-house, having two halves machined in methacrylate polymer, each with a volume of approximately 5 mL (see Figure 3.1). The two halves were separated by a dialysis membrane held in place by two Teflon gaskets on either side. Samples were inserted and removed for analysis via a threaded hole located in the top of each half, and kept sealed with a stainless steel screw during the experiment.

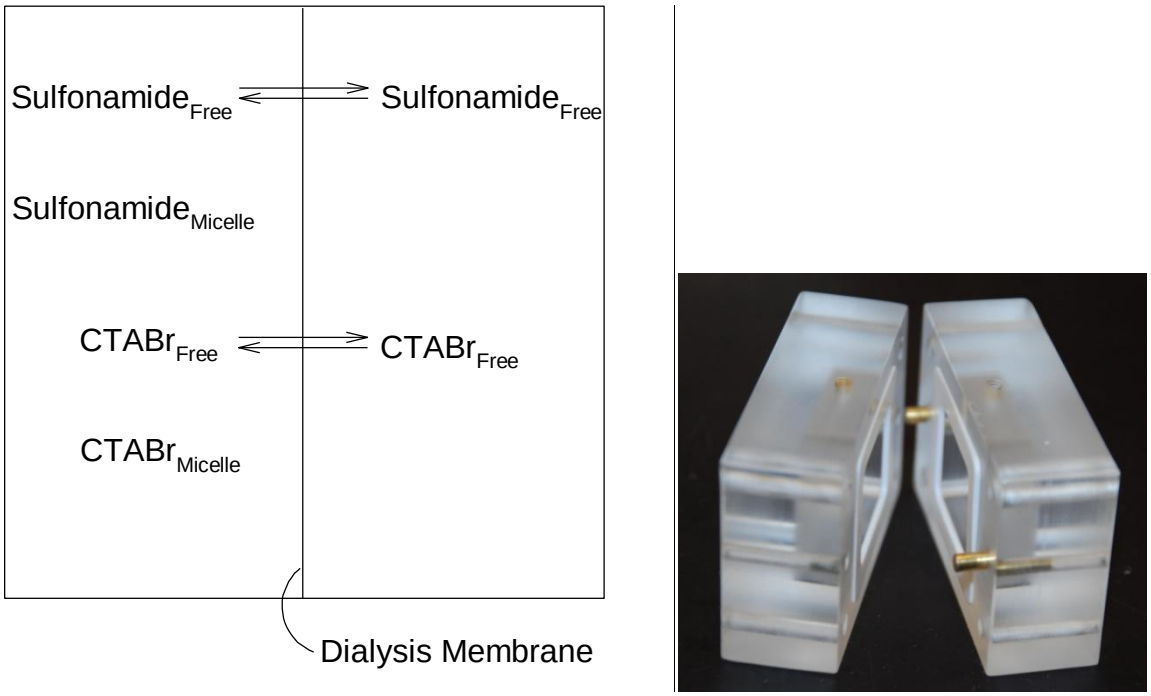

Figure 3.1 Schematic of SED Cell Operation

3.2.2 Solution Preparation

Standard solutions of sulfonamides used for SED analysis were prepared from a stock solution made by addition of the appropriate amount of sulfonamide in 100 mL H_2O, followed by sonication at 35°C to aid dissolution. Samples were sonicated again prior to use.

Sulfonamide	Molecular Weight ($g \cdot mol^{-1}$)	Mass Added (g)	Amount Added (mol)	Molarity (M)
Sulfacetamide (1)	214.24	0.0023	$1.1x10^{-5}$	$1.1x10^{-4}$
Sulfadiazine (2)	250.28	0.0025	$1.0x10^{-5}$	$1.0x10^{-4}$
Sulfaguanidine (3)	214.24	0.0026	$1.2x10^{-5}$	$1.2x10^{-4}$
Sulfamerazine (4)	264.31	0.0028	$1.1x10^{-5}$	$1.1x10^{-4}$
Sulfamethoxazole (5)	253.28	0.0026	$1.1x10^{-5}$	$1.1x10^{-4}$
Sulfathiazole (6)	255.32	0.0026	$1.1x10^{-5}$	$1.1x10^{-4}$

CTABr solutions were prepared via serial dissolution of a 2.00×10^{-2} M CTABr stock solution prepared by dissolving 0.7275 g of CTABr (MW = 364.45 $g \cdot mol^{-1}$) in 100 mL H_2O. Dissolution was aided by placing the solution in an ultrasonic bath at 35°C for 30 minutes. Prior to further use, CTABr stock solutions were sonicated again, as precipitate would often form if solutions were left at room temperature for a period longer than one day.

3.2.3 Semi-equilibrium Dialysis

On one side of the equilibrium dialysis cell, 4.0 mL of deionized water was added and on the other, 2.0 mL of the sulfonamide solution and 2.0 mL of the CTABr solution, resulting in a total volume of 4.0 mL on each side of the dialysis membrane. Initial CTABr concentrations in the retentate were one half that of the stock solution, whereas three different initial retentate sulfonamide concentrations were utilized – a 1:2 dilution of the stock, a 1:20 dilution of the stock, and finally, a 1:200 dilution of the stock, so as to ensure that LC-MS/MS analysis could be performed successfully regardless of the binding constant. The dialysis membrane used was hydrated in Milli-Q water for two minutes prior to use.

Cells were allowed to equilibrate for 24 h, at which point 2.5 mL of sample was removed from each side and analyzed by LC-MS/MS and conductivity. Equilibration times were determined by performing an experiment where either sulfonamide or CTABr alone was added to the retentate, and the concentrations checked after 24 h. Solutions were considered to be semi-equilibrated when

permeate and retentate concentrations of sulfonamide were equal, and when the permeate concentration of CTABr was equal to the C_{CMC} for the surfactant.

Following use, cells were cleaned with deionized water and dried with a laboratory wipe a minimum of four times, followed by drying under nitrogen prior to the next use.

Binding constants were generated by analysis of permeate and retentate concentrations of sulfonamide and CTABr; however due to large differences between permeate and retentate concentrations only the trial consisting of the most concentrated sulfonamide solution could be analyzed.

3.2.4 LC-MS/MS Analysis

Sulfonamide concentrations were determined by a method similar to that employed by Balakrishnan et al.[6] on a Quattro Ultima tandem LC triple quadrupole mass spectrometer (Micromass, Manchester, UK) with samples introduced via electrospray ionization operated in positive ion mode. Nitrogen was used as both drying and nebulizing gas at flowrates of 500 L/h and 70 L/h, respectively. Collision induced dissociation was performed using argon in a hexapole collision cell. MassLynx software (Waters Corporation, Milford, USA, v4.1) was used for acquisition and analysis of spectra, with the MS operated in multiple reaction monitoring (MRM) mode. A dwell time of 100 ms and interchannel delay of 50 ms were used.

Separation was achieved by using a Waters Acquity Ultra Performance LC system. An XTerra C18 5µm, 2.1mm x 250mm column was utilized. 5 µL was

injected onto the column, and elution was performed with a flowrate of 0.2 mL/min, with two solvents being used – Solvent A was composed of a 2:1 acetonitrile:methanol 20 mM NH_4Ac buffer, and Solvent B a 20mM NH_4Ac 0.1% formic acid solution. The initial gradient was 98% B, which was decreased to 50% B over twelve minutes, and eventually 0% B by thirteen minutes. 0% B was held until twenty-three minutes, where the solvent was switched to 98% B over one minute, and held until thirty minutes. The source temperature was 120°C, and the desolvation temperature 350°C.

Prior to analysis, samples were diluted by a factor of 1:10 with Milli-Q water. Samples were positively identified by retention time and product ion analysis. Table 3.2 below shows the applicable retention times and mass transitions, and Figure 3.2 an example chromatogram.

Table 3.2 Retention Time and Mass Transitions for Studied Sulfonamides

Compound	Retention Time (min)	Precursor Ion $[M+H]^+$ (*m/z*)	Product Ion (*m/z*)
1	8.3	215	156
2	9.0	251	156
3	5.7	215	156
4	10.1	265	156
5	12.8	254	156
6	9.5	256	156

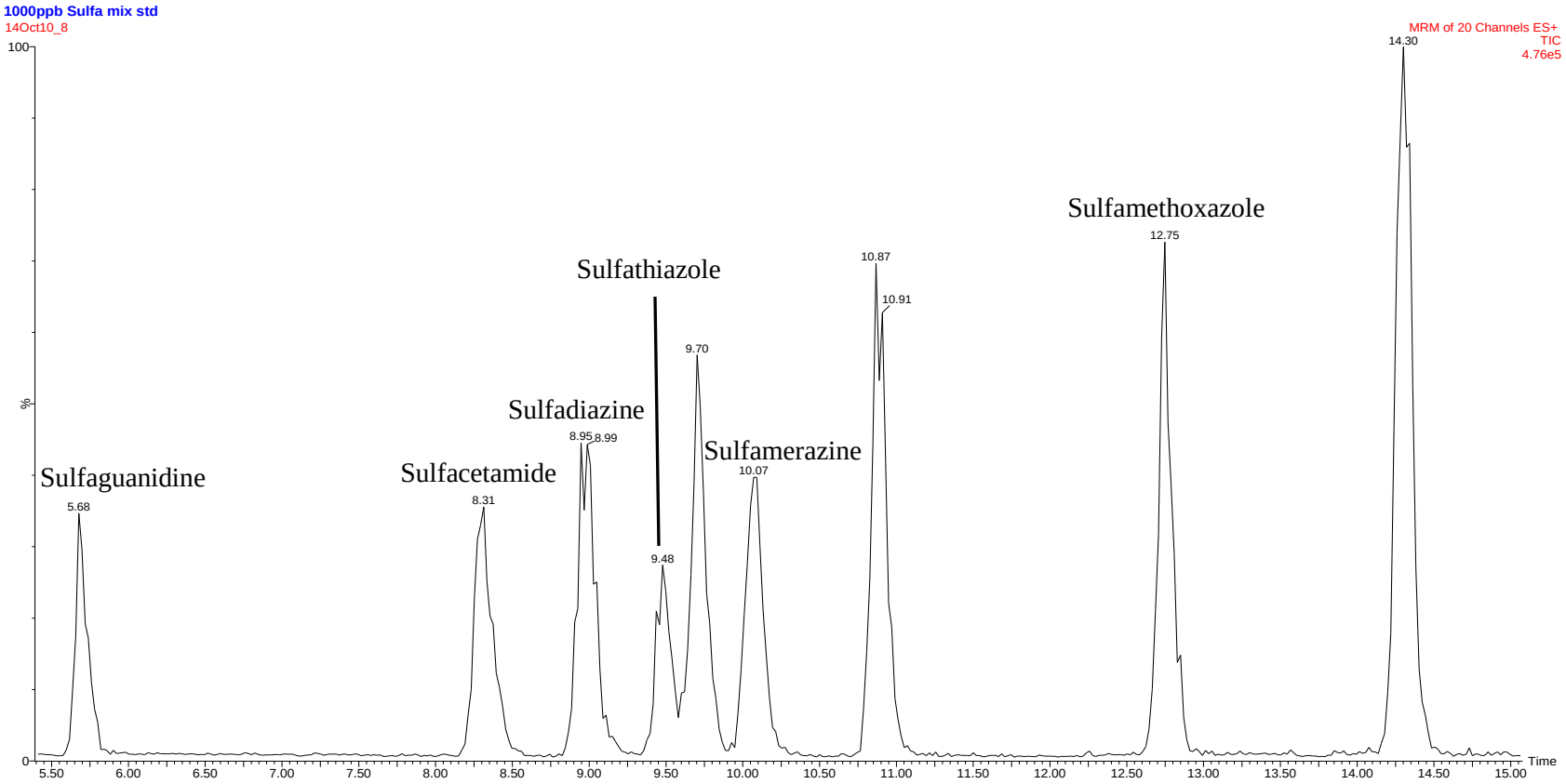

Figure 3.2 Example Chromatogram for Analysis of Nine Sulfonamides

(Note: The method used generates calibration curves for nine sulfonamide analogs shown above. Only six are analyzed in this work.)

3.2.5 Conductivity Analysis

CTABr in the permeate and retentate was quantified by conductivity of the respective solutions compared to a calibration curve ranging from $2x10^{-3}$ to $2x10^{-4}$ M. Solutions were diluted by a factor of 1:10 prior to analysis. Conductivity was determined with a Jenway 470 Conductivity Meter. Samples with conductivity lower than 60 μS were correlated with the first portion of the curve, and samples with a conductivity higher than 60 μS correlated with the latter portion.

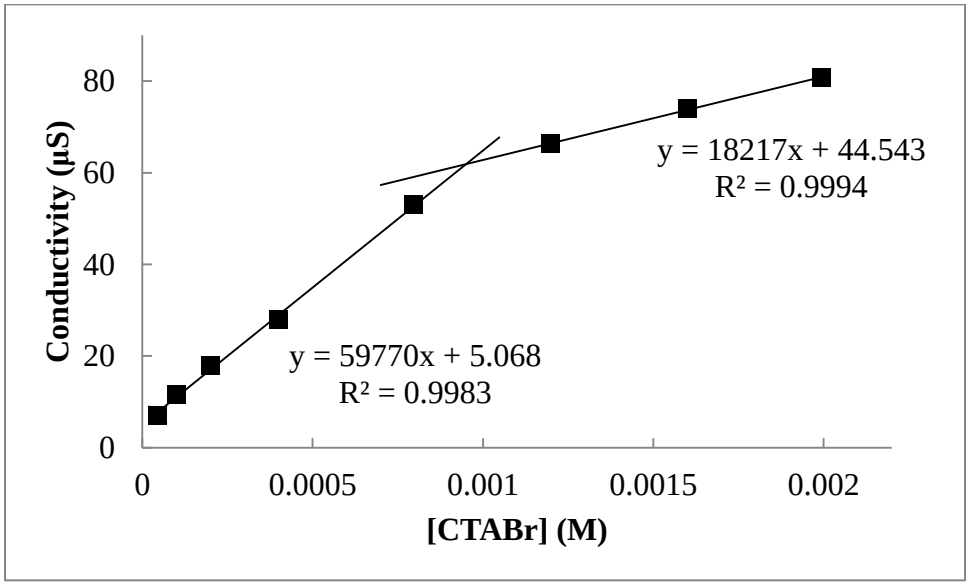

Figure 3.3 Calibration Curve for Determination of [CTABr] by Conductivity

3.3 Results & Discussion

3.3.1 Binding Constants

LC-MS/MS analysis provided useable results (i.e. within the calibration range) for only the first series of sulfonamide samples where [Sulfonamide] was approximately $5x10^{-5}$ M. It was noted that mass balance was not achieved – that is, the amount of sulfonamide and surfactant added did not equal the sum of the sulfonamide and surfactant present in the permeate and retentate. This would seem to indicate that some of the sulfonamide and surfactant partition to the membrane itself, which has been demonstrated previously[18].

Conductivity analysis showed that the permeate concentration of CTABr was consistent between samples while concentrations in the retentate varied. Interestingly, the retentate concentration of surfactant was always greater than the C_{CMC}, however it is unlikely that the concentrations of sulfonamide utilized would have any major impact on the C_{CMC}.

Binding constants were determined in each case by the application of Equation 3.1. Table 3.3 below shows the final concentrations of surfactant and sulfonamide in each of the permeate and retentate after 24 h.

Table 3.3 Concentrations of SED Experiments After 24h With Corresponding log(K_B)

Compound	log(K_{OW})	$[CTABr]_R$ (M)	$[CTABr]_P$ (M)	$[Sulfonamide]_R$ (M)	$[Sulfonamide]_P$ (M)	log(K_B)
Sulfacetamide	-0.96	$5.09x10^{-3}$	$8.00x10^{-4}$	$4.07x10^{-5}$	$6.20x10^{-6}$	4.30
Sulfadiazine	-0.09	$5.17x10^{-3}$	$6.79x10^{-5}$	$1.42x10^{-5}$	$2.51x10^{-6}$	4.20
Sulfaguanidine	-1.22	$4.91x10^{-3}$	$1.00x10^{-3}$	$1.88x10^{-5}$	$1.48x10^{-5}$	3.05
Sulfamerazine	0.14	$4.31x10^{-3}$	$7.11x10^{-4}$	$1.24x10^{-5}$	$2.14x10^{-6}$	4.42
Sulfamethoxazole	0.89	$5.24x10^{-3}$	$7.76x10^{-4}$	$1.35x10^{-5}$	$2.59x10^{-7}$	5.24
Sulfathiazole	0.05	$4.96x10^{-3}$	$8.08x10^{-4}$	$2.22x10^{-5}$	$3.84x10^{-7}$	5.34

Binding constants were expected to follow a trend with K_{OW}, and so a log-log plot was produced in an attempt to correlate the binding constants with K_{OW}.

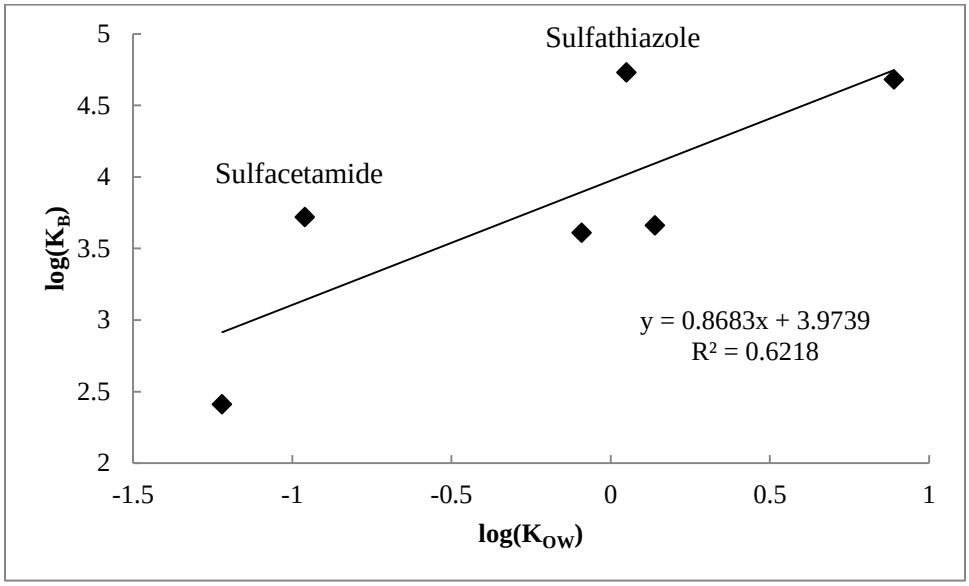

Figure 3.4 Plot of $\log(K_B)$ vs. $\log(K_{OW})$ for Six Sulfonamides

(Note: $\log(K_B)$ and $\log(K_{OW})$ values taken from Table 3.3)

Clearly a trend exists between K_{OW} and K_B, however as shown by the relatively low correlation coefficient ($R^2 = 0.6218$) there are other factors contributing to the binding constant. This is perhaps to be expected, as molecules partitioning between a micelle and water are driven not only by hydrophobic effect optimization, but also by interaction with the charged layer.

Any description of the interaction of a sulfonamide and a micelle must include these two factors. Since K_{OW} acts only as a surrogate for the hydrophobic effect, any predictive system should also attempt to account for electrostatic interactions of the charged layer and the individual sulfonamides. This is particularly true for sulfacetamide and sulfathiazole, which suggests some additional binding other than purely hydrophobic interactions.

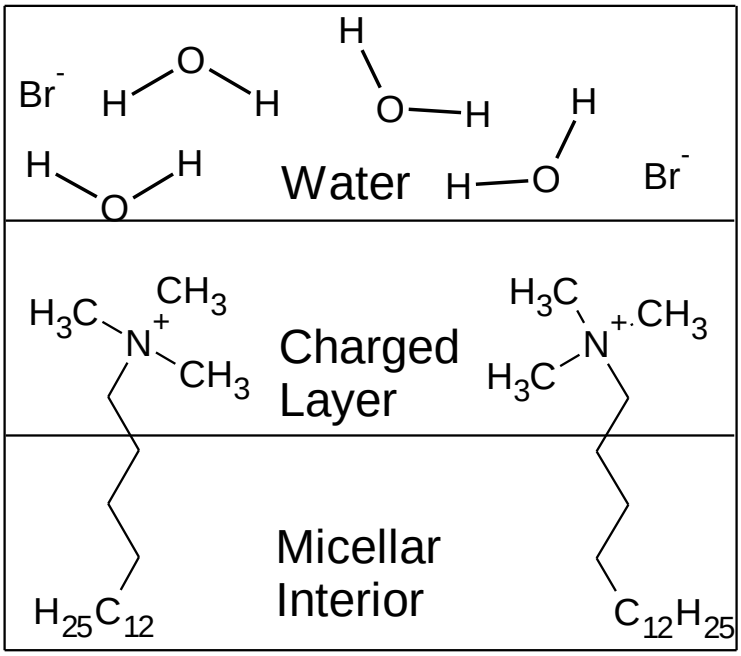

Figure 3.5 Cross-sectional Representation of a Micelle

3.3.2 Gibbs Free Energy of Transfer Analysis

Binding constants determined by the methods outlined in above and in Chapter 2 are tabulated below in Table 3.4. It is apparent that SED binding constants are higher than those determined by ^{1}H NMR, however NMR values are in fact taken as the average of the binding constants determined from each individual proton in the analog. Thus, for subsequent analysis, the SED binding constants are used.

Table 3.4 Binding Constants for Seven Sulfonamides as Determined by Two Methods

	log(K_B)	
Compound	NMR	SED
Sulfacetamide	3.84	4.30
Sulfanilamide	<2.5	N/A
Sulfadiazine	3.81	4.20
Sulfaguanidine	<2.5	3.05
Sulfamerazine	4.11	4.42
Sulfamethoxazole	4.35	5.24
Sulfathiazole	3.12	5.34

Using the SED binding constants, application of Equation 3.2 results in the generation of a series of change in Gibbs free energy for the transfer from solution to the micelle, as shown below in Table 3.5.

Table 3.5 Change in Gibbs Free Energy for Micellar Inclusion of Six Sulfonamides

Compound	log(K_B)	ΔG^0
Sulfacetamide	4.30	-24.6
Sulfadiazine	4.20	-24.0
Sulfaguanidine	3.05	-17.4
Sulfamerazine	4.42	-25.2
Sulfamethoxazole	5.24	-29.9
Sulfathiazole	5.34	-30.5

It is known that aniline will partition to CTABr, predominantly as a result of hydrophobic effect interactions as well as cation-pi interactions between the aromatic ring and the trimethylammonium headgroups. From Table 3.1, it can be said that an aniline moiety partitioning to CTABr has a free energy change of -7.7

kJ/mol. If we treat the Gibbs free energy change of partitioning as an additive function, then since all the sulfonamides examined contain a p-aniline moiety bonded to the sulfur of the sulfonamide linkage, inferences may be made regarding the contribution of the sulfonamide linkage and additional moiety to the overall binding phenomenon.

It is of interest to first determine the contribution of the sulfonamide linkage itself. Sulfaguanidine shows the smallest binding constant, and so is ideal to begin the examination. Guanidine itself is mostly charged and quite hydrophilic, having a $pK_b = 1.5$, and so can be expected not to contribute to the binding. Thus, the remainder of the change in free energy on partitioning arises from the contributions of the sulfonamide linkage and p-aniline moiety. From this, we can thus calculate that the contribution of the sulfonamide linkage partitioning to a CTABr micelle is approximately -9.5 kJ/mol due to cation-dipole interactions and the hydrophobic effect, the difference between the binding constant determined for sulfaguanidine and that of aniline.

Sulfacetamide shows a change in free energy of -24.6 kJ/mol, indicating that if the sulfonamide linkage contributed -9.5 kJ/mol and the aniline group -7.7 kJ/mol then the acetyl group contributes approximately -7.4 kJ/mol. This seems somewhat high at first, however the following resonance structure can be considered:

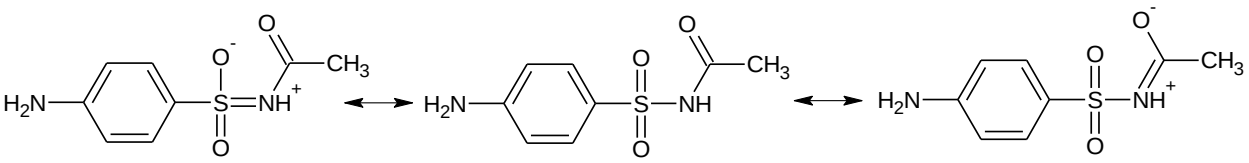

In the zwitterionic form shown above on the right, an oxygen anion is present. If this is a dominant resonance form, it could contribute at least -7 kJ/mol due to the anionic oxygen as suggested in Table 3.1, as well as the contribution from the hydrophobic effect on inclusion of the methyl group into the micellar interior. The presence of nearby trimethylammonium headgroups could promote this form and make the zwitterionic form more prevalent. Quantitative analysis is, however, quite difficult at this point as the exact distribution of resonance forms is unknown, however the unusually high binding constant for a compound with such a low K_{OW} would seem to be indicative of other non-hydrophobic effect binding such as ion-ion interactions.

In the case of sulfadiazine, the pyrimidine moiety contributes -6.8 kJ/mol. whereas in sulfamerazine the methylpyrimidine contribution is -8.0 kJ/mol. From this the contribution of the additional methyl group is calculated to be -1.2 kJ/mol towards the free energy change. This is slightly less than the -2 kJ/mol reported in the literature for addition of a p-methyl to benzoic acid or phenol[11]. Unfortunately, no values are available for the partitioning of either a pyridine or pyrimidine group to a micelle.

Calculations for the contribution of methoxazole and thiazole groups to the change in free energy indicates a change of approximately -13 kJ/mol. Since cation-pi interactions are not possible in the same sense as for the pyrimidine compounds, this would suggest that the hydrophobic effect would have a greater influence on the binding of sulfamethoxazole and sulfathiazole. However, sulfathiazole has a very small log(K_{OW}) of 0.05 but a large log(K_B) of 5.34, and sulfamethoxazole has a larger log(K_{OW}) of 0.89 and a large log(K_B) of 5.24. While the slightly higher log(K_{OW}) can explain the increased binding constant of sulfamethoxazole, the overall log(K_B) values cannot be explained by the log(Kow) values. Other interactions between these compounds and the micelles must be occurring to account for the behavior of sulfathiazole and sulfamethoxazole.

The calculations of change in Gibbs free energy generally support the orientation and locus proposed for association with the micelle in Chapter 2; however it is now possible to propose a modification of the orientation and locus proposed for sulfacetamide based upon examination of the binding constant.

Changes in Gibbs free energy indicated that the binding constant could be enhanced by the presence of an oxygen anion coordinating with the trimethylammonium headgroup. In Chapter 2, no additional resonance forms were considered, and all molecules were assumed to be in their neutral state as suggested by their respective values of pK_a. However, as suggested,

sulfacetamide may exist in its zwitterionic form and so the following modification of Figure 2.6 can be proposed.

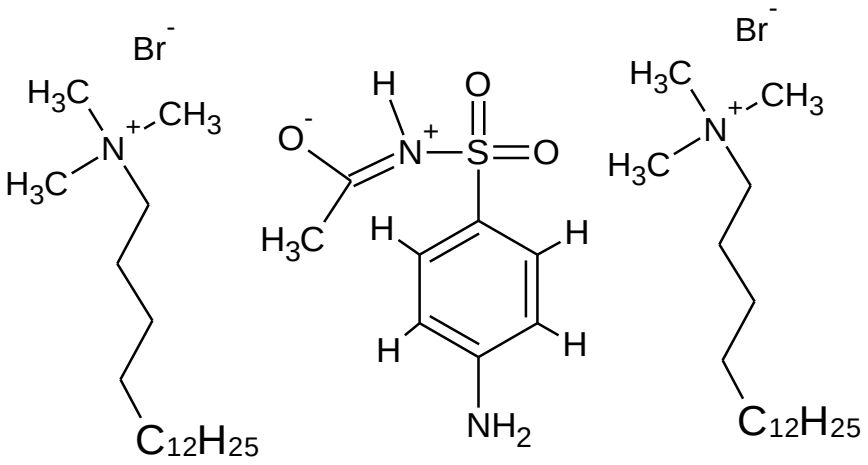

Figure 3.6 Proposed Modified Association of Sulfacetamide with a CTABr Micelle

The modification does not change the proposed orientation and locus greatly, merely the electronic structure of sulfacetamide within the micelle. If the two potential electronic structures are in equilibrium, many literature reports detail how equilibrium constants are affected by micellar systems[16]. One potential implication of the zwitterionic state of sulfacetamide is that it will be located closer to the exterior of the micelle, as has been shown for other species with an anionic oxygen[17]. In most other systems examined by both NMR and SED, this is not an issue, as changes in free energy calculations are consistent with the orientation and locus previously proposed, where hydrophobic groups are located within the interior of the micelle and the sulfonamide linkage is located within the charged layer.

3.4 Conclusions

SED experiments have provided an alternative means to evaluate binding constants without many of the limitations imposed by NMR measurements previously employed. There is a correlation between K_{OW} and binding constant, however this correlation itself is not strong enough to allow for prediction of K_B from K_{OW} values at this time, due to the various mechanisms by which molecules are able to interact with aqueous micelles. Thus, development of a structure-activity relationship must take into account more than just K_{OW}, but also potential electrostatic interactions that occur with the charged layer.

Accurate determination of binding constants can also shed light on the mechanisms of binding; the binding constant can be seen as a measure of the change in free energy arising from the association of the sulfonamide with the micelle, and differences between analogs indications of variation in the binding mechanism and thus orientation and locus within the micelle itself.

Examination of the change in free energy from partitioning supports the orientations proposed by ^{1}H NMR studies in Chapter 2, where for most sulfonamides the entire molecule is inside the micelle. For sulfaguanidine, the guanidine moiety is determined to be located exterior to the charged layer of the micelle.

Further examination of the change in free energy allows for the proposed of certain binding mechanisms, such as that seen in sulfacetamide, where the unexpectedly high binding constant may be the result of a resonance structure

allowing for the coordination of an additional potential anionic oxygen with the cationic trimethylammonium headgroup. Unfortunately, examination of free energies is unable to explain all the binding behavior seen, such as that for sulfathiazole.

As such, attempts to characterize the orientation and locus of a compound within a micelle should whenever possible take into account the specific interactions that contribute to partitioning by examination of binding constants. This will ensure that in scenarios where binding other than hydrophobic effect interactions or similar cation-pi interactions are occurring, such behavior may be fully elucidated.

3.5 References

(1) Dunn, R. O.; Scamehorn, J. F.; Christian, S. D. *Sep. Sci. Technol.* **1985**, *20*, 257.

(2) Rouse, J. D.; Sabatini, D. A.; Deeds, N. E.; Brown, R. E.; Harwell, J. H. *Environ Sci Technol* **1995**, *29*, 2484.

(3) Ergican, E.; Gecol, H. *J Membrane Sci* **2008**, *325*, 69.

(4) Nesmerak, K.; Nemcova, I. *Anal Lett* **2006**, *39*, 1023.

(5) Bhat, P. A.; Dar, A. A.; Rather, G. M. *J Chem Eng Data* **2008**, *53*, 1271.

(6) Balakrishnan, V. K.; Terry, K. A.; Toito, J. *J Chromatogr A* **2006**, *1131*, 1.

(7) IUPAC In *Compendium of Chemical Terminology*; 2nd ed.; Blackwell Scientific Publications: 1997.

(8) Pramauro, E.; Minero, C.; Saini, G.; Graglia, R.; Pelizzetti, E. *Anal Chim Acta* **1988**, *212*, 171.

(9) Atkins, P. W.; De Paula, J. *Atkins' Physical chemistry*; 8th ed.; W.H. Freeman: New York, 2006.

(10) Bunton, C. A.; Sepulveda, L. *J Phys Chem* **1979**, *83*, 680.

(11) Hirose, C.; Sepulveda, L. *J Phys Chem* **1981**, *85*, 3689.

(12) Gamboa, C.; Sepulveda, L.; Soto, R. *J Phys Chem* **1981**, *85*, 1429.

(13) Gao, J.; Chou, L. W.; Auerbach, A. *Biophys J* **1993**, *65*, 43.

(14) Bunton, C. A.; Minch, M. J. *J Phys Chem* **1974**, *78*, 1490.

(15) Pramauro, E.; Saini, G.; Pelizzetti, E. *Anal Chim Acta* **1984**, *166*, 233.

(16) Vlasenko, A. S.; Loginova, L. P.; Iwashchenko, E. L. *J Mol Liq* **2009**, *145*, 182.

(17) Sabatino, P.; Szczygiel, A.; Sinnaeve, D.; Hakimhashemi, M.; Saveyn, H.; Martins, J. C.; Van der Meeren, P. *Colloids and Surfaces A: Physicochemical and Engineering Aspects* **2010**, *370*, 42.

(18) Majewska-Nowak, K.; Kowalska, I.; Kabsch-Korbutowicz, M. *Desalination* **2006**, *198*, 149.

Chapter 4

Conclusions and Future Work

4.1 Conclusions

Studies performed via ^{1}H NMR spectroscopy suggest that sulfonamide antibiotics will partition to aqueous CTABr micelles in various ways, with studied analogs falling into one of two categories. Sulfonamides with a hydrophobic moiety on either side of the linkage partition with the hydrophobic portions oriented towards the interior, less polar region of the micelle, while the sulfonamide linkage coordinates with the cationic trimethylammonium headgroups of CTABr. Analogs without two hydrophobic moieties (i.e. sulfanilamide and sulfaguanidine) show weak coordination, with minimal penetration of the hydrophilic moiety into the surface and weak coordination of the sulfonamide linkage.

^{1}H NMR chemical shift results were also used to calculate binding constants. For some analogs the chemical shift was insufficiently large to allow for accurate binding constant determination, and for other analogs binding constants ranged over an order of magnitude between protons.

To overcome the deficiencies of ^{1}H NMR analysis for binding constants, SED experiments were performed to determine binding constants. The binding constants generated by SED were generally higher than those generated from ^{1}H

NMR. These binding constants were then converted to measures of change in free energy, and the relative contribution of various moieties calculated. Such analysis generally confirmed the orientation and locus proposed by ^{1}H NMR, with the exception of sulfacetamide where a slight change was required to the proposed orientation.

It was found that there is a correlation between binding constant and octanol-water partition coefficient, however there were at least two cases (sulfacetamide and sulfathiazole) for which the correlation was weak. For sulfacetamide, the discrepancy can be explained by an additional binding mechanism that adds greatly to the binding constant. As such, unless other specific intermolecular interactions are present, octanol-water partition coefficient should allow for a rough estimate of binding constants.

4.2 Future Work

4.2.1 Orientation, Locus, and Binding Constant

The orientation and locus of binding were predicted as a result of ^{1}H NMR CTABr titration type experiments, however more advanced NMR pulse sequences such as NOESY should allow for elucidation of the specifics of the binding more carefully. Such experiments were attempted but failed to generate usable data for our system. More detailed analysis may provide results for new systems with higher power instruments. As well, NMR experiments to determine diffusion coefficients could be used to evaluate binding constants more

accurately *in situ*. Evaluation of additional, accurate binding constants when combined with orientation and locus data could then be used to generate a more accurate predictive system than demonstrated in this work, one that uses a combination of factors such as octanol-water partition coefficient as well as factors such as the Kamlet-Taft solvatochromic parameters.

4.2.2 Remediation & Removal Efficiency

To date, all work has been focused on evaluation of binding constants and orientation. Actual MEUF experiments should be performed to determine removal efficiencies for selected compounds so that a comparison can be made between binding constants and removal efficiencies.

Additionally, the studied compounds should be expanded upon to include not only sulfonamides, but other classes of pharmaceuticals and water contaminants that are not efficiently removed by current water treatment methodologies.

Appendix A

NMR Assignments

Sulfacetamide ^{1}H NMR (500 MHz, D_2O)

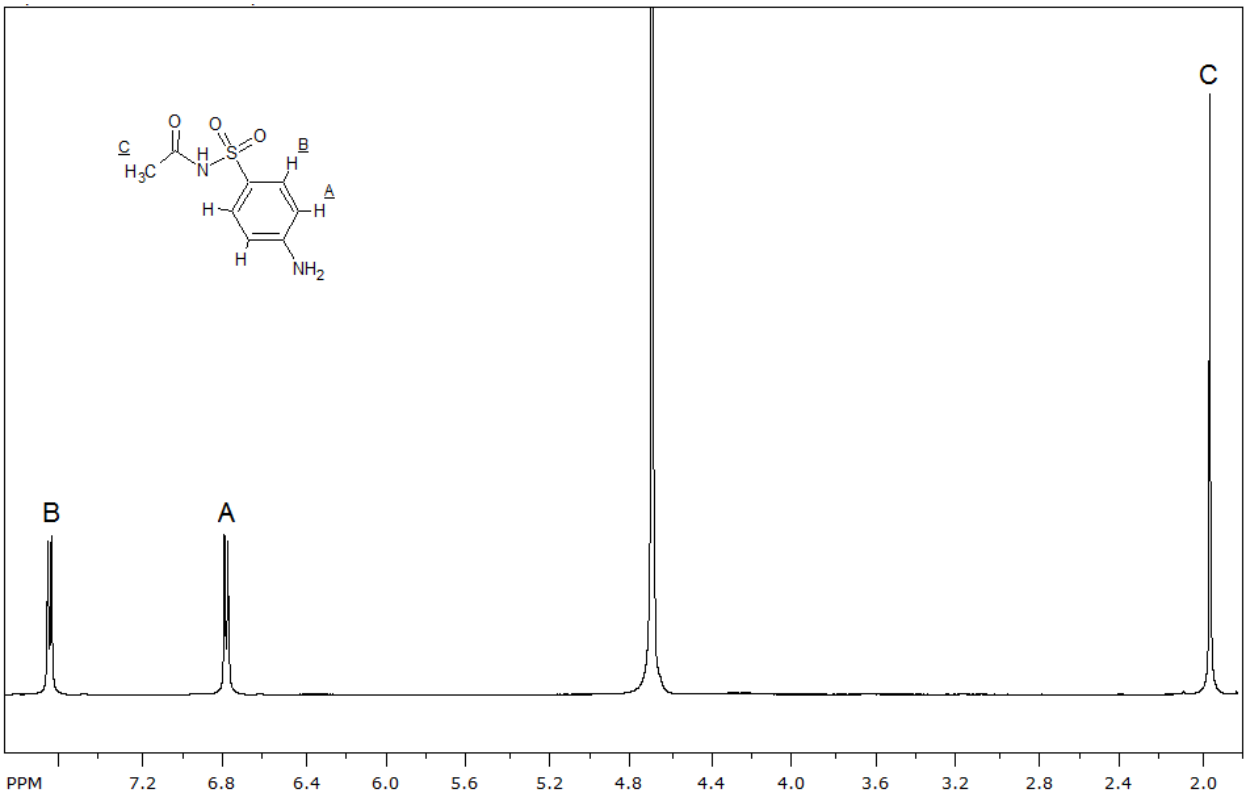

A: δ = 6.789 ppm, d, J_{A-B} = 8.8 Hz

B: δ = 7.658 ppm, d, J_{A-B} = 8.8 Hz

C: δ = 1.951 ppm, s

Sulfanilamide ^{1}H NMR (500 MHz, D_2O)

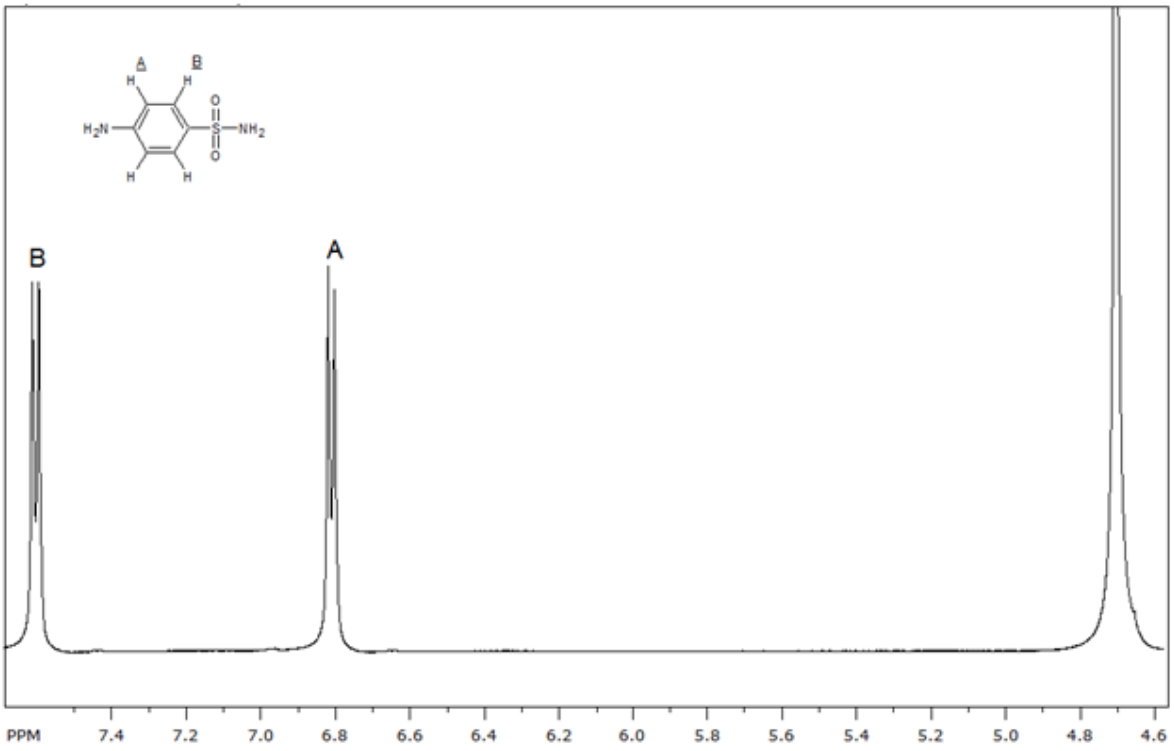

A: δ = 6.812 ppm, d, $J_{A\text{-}B}$ = 8.8 Hz

B: δ = 7.608 ppm, d, $J_{A\text{-}B}$ = 8.8 Hz

Sulfadiazine ^{1}H NMR (500 MHz, D_2O)

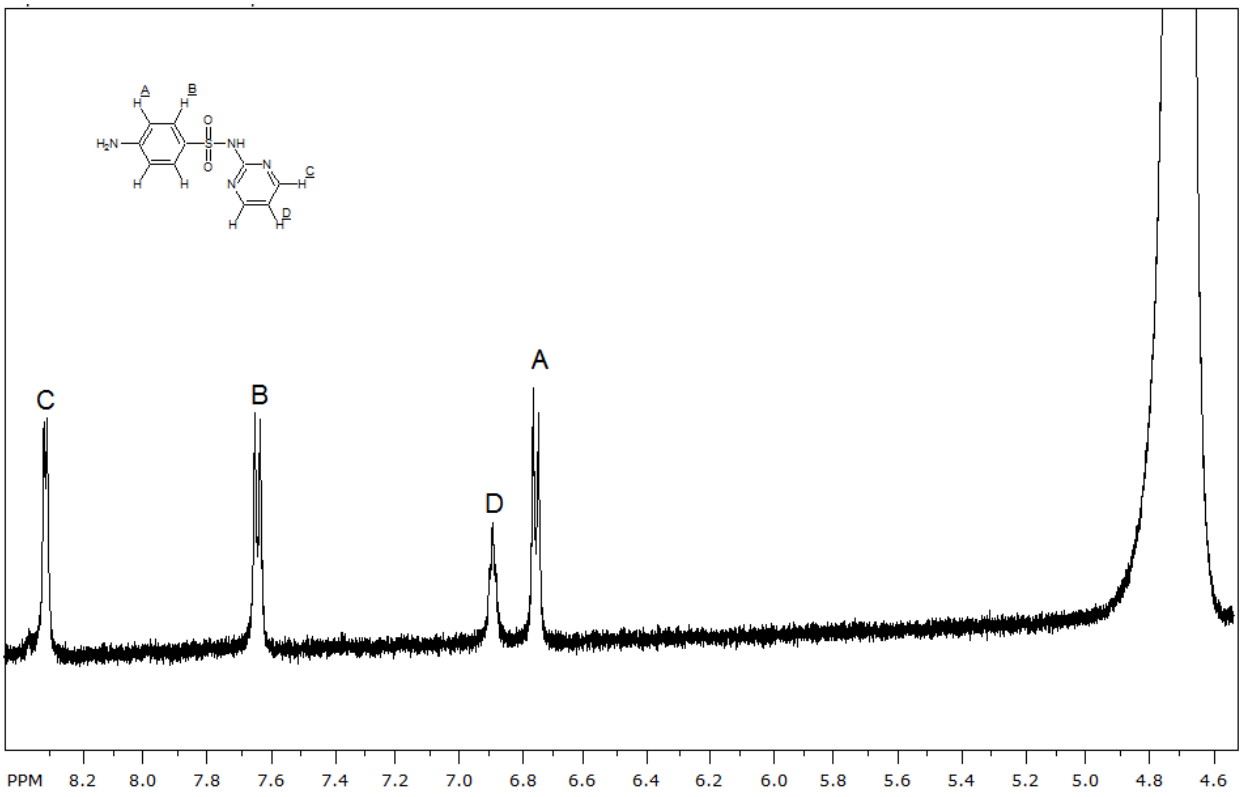

A: δ = 6.758 ppm, d, J_{A-B} = 8.7 Hz

B: δ = 7.648 ppm, d, J_{A-B} = 8.7 Hz

C: δ = 8.325 ppm, d, J_{C-D} = 5.0 Hz

D: δ = 6.896 ppm, t, J_{C-D} = 5.0 Hz

Sulfadoxine ^{1}H NMR (500 MHz, D_2O)

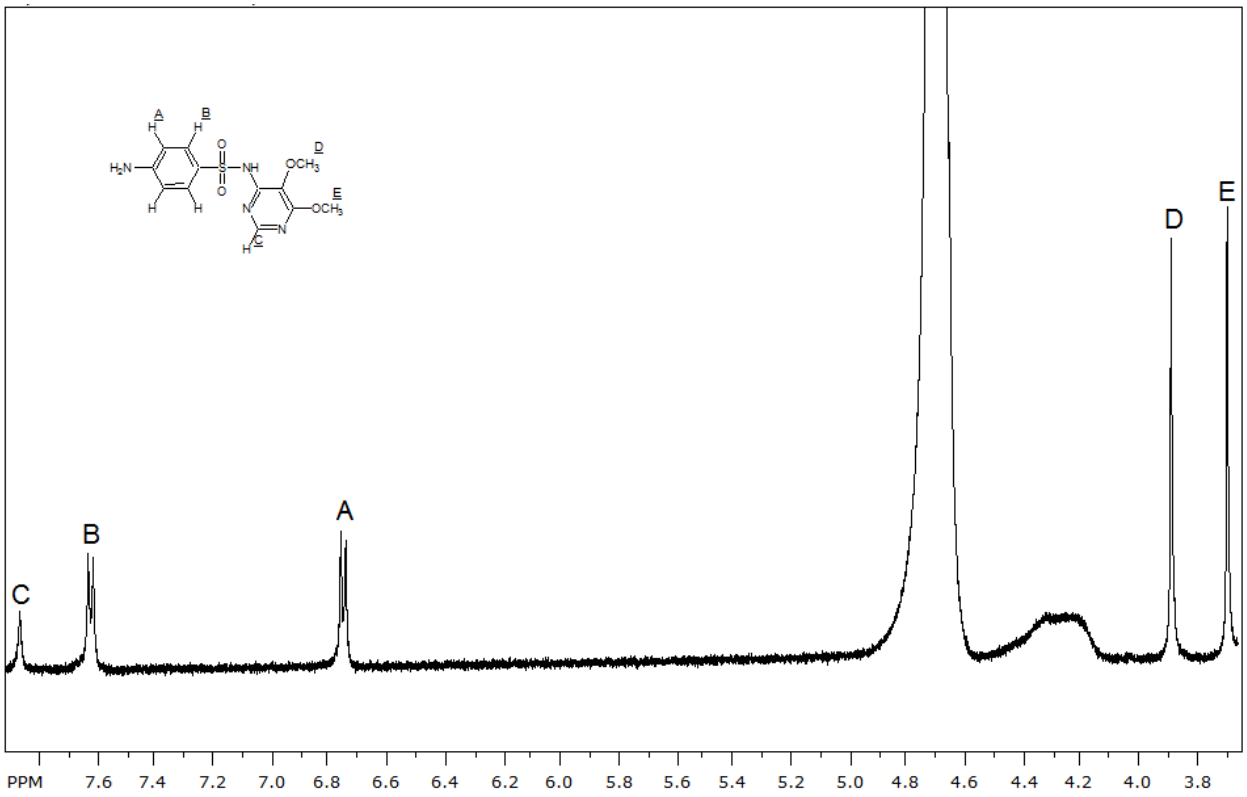

A: δ = 6.755 ppm, d, $J_{A\text{-}B}$ = 8.6 Hz

B: δ = 7.630 ppm, d, $J_{A\text{-}B}$ = 8.6 Hz

C: δ = 3.689 ppm, s

D: δ = 3.883 ppm, s

E: δ = 7.876 ppm, s

Sulfaguanidine ^{1}H NMR (500 MHz, D_2O)

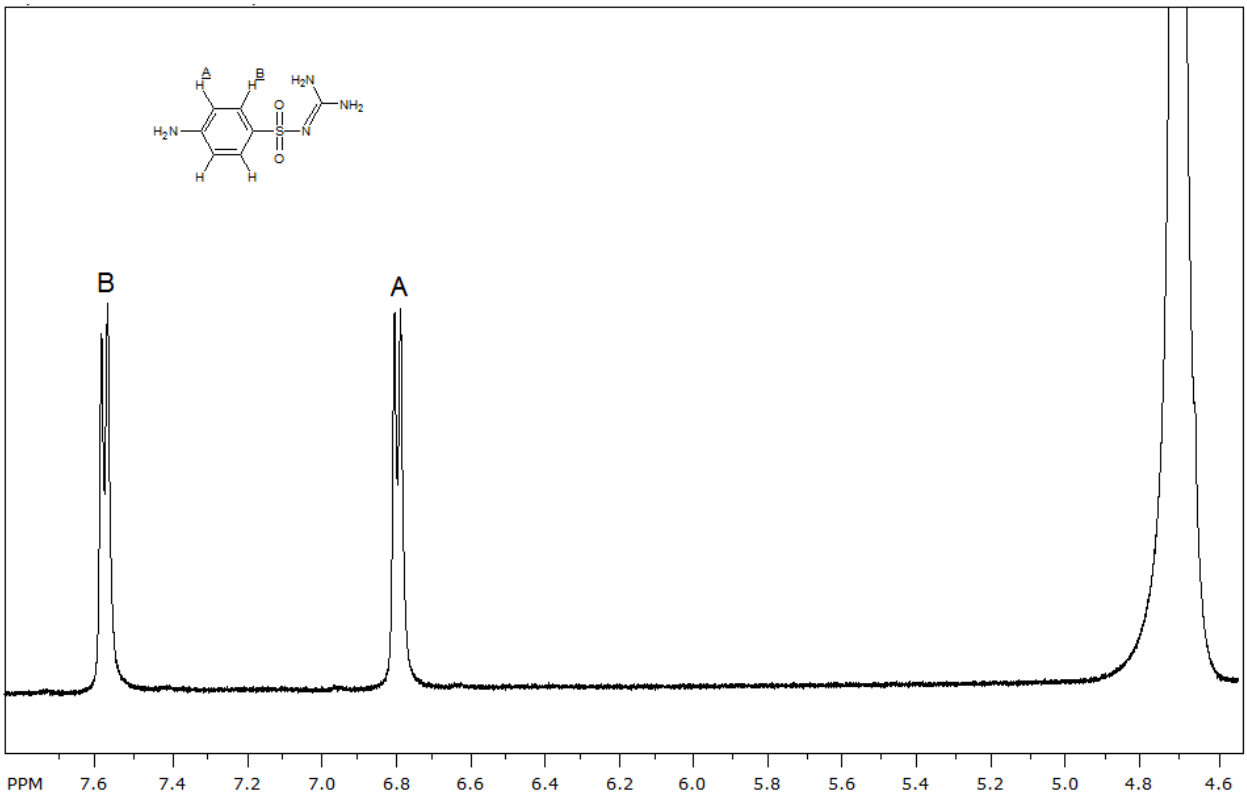

A: δ = 6.797 ppm, d, $J_{A\text{-}B}$ = 8.7 Hz

B: δ = 7.583 ppm, d, $J_{A\text{-}B}$ = 8.7 Hz

Sulfamerazine ^{1}H NMR (500 MHz, D_2O)

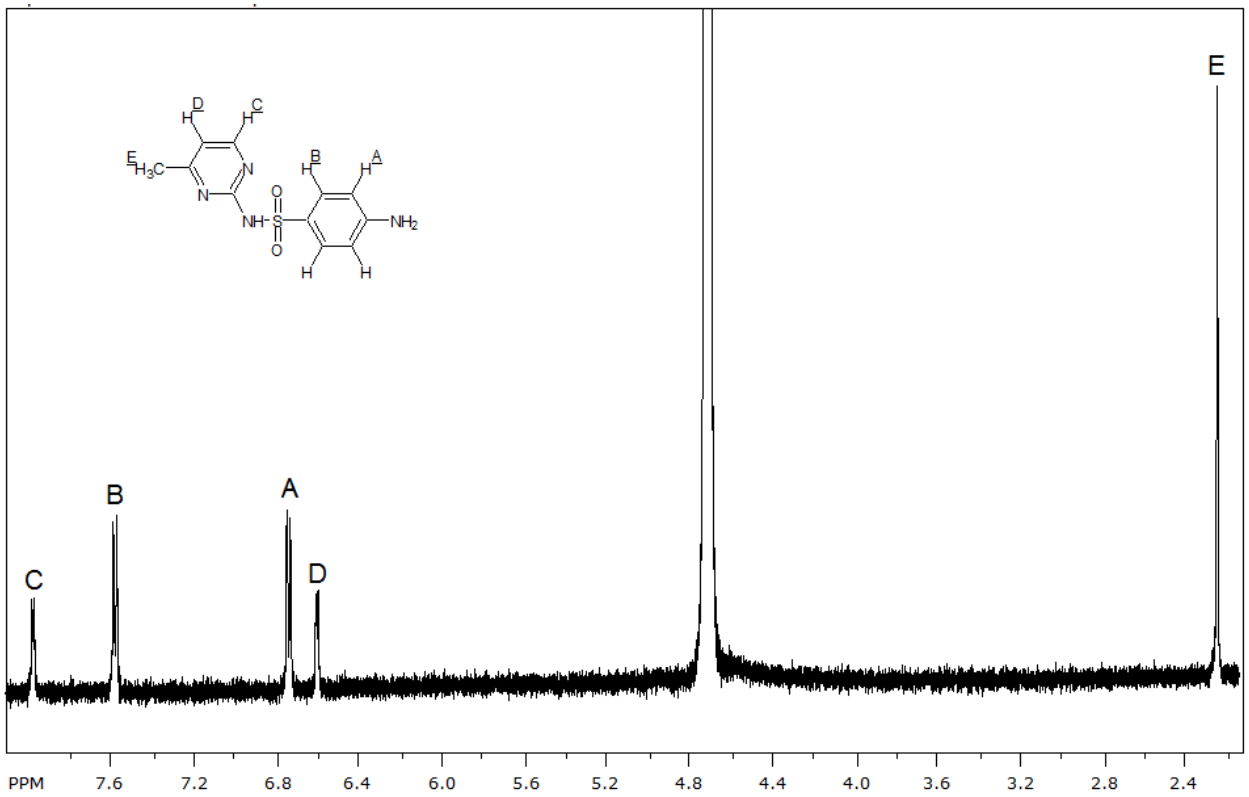

A: δ = 6.752 ppm, d, J_{A-B} = 8.7 Hz

B: δ = 7.596 ppm, d, J_{A-B} = 8.7 Hz

C: δ = 7.996 ppm, d, J_{C-D} = 5.1 Hz

D: δ = 6.615 ppm, d, J_{C-D} = 5.1 Hz

E: δ = 2.235 ppm, s

Sulfamethazine ^{1}H NMR (500 MHz, D_2O)

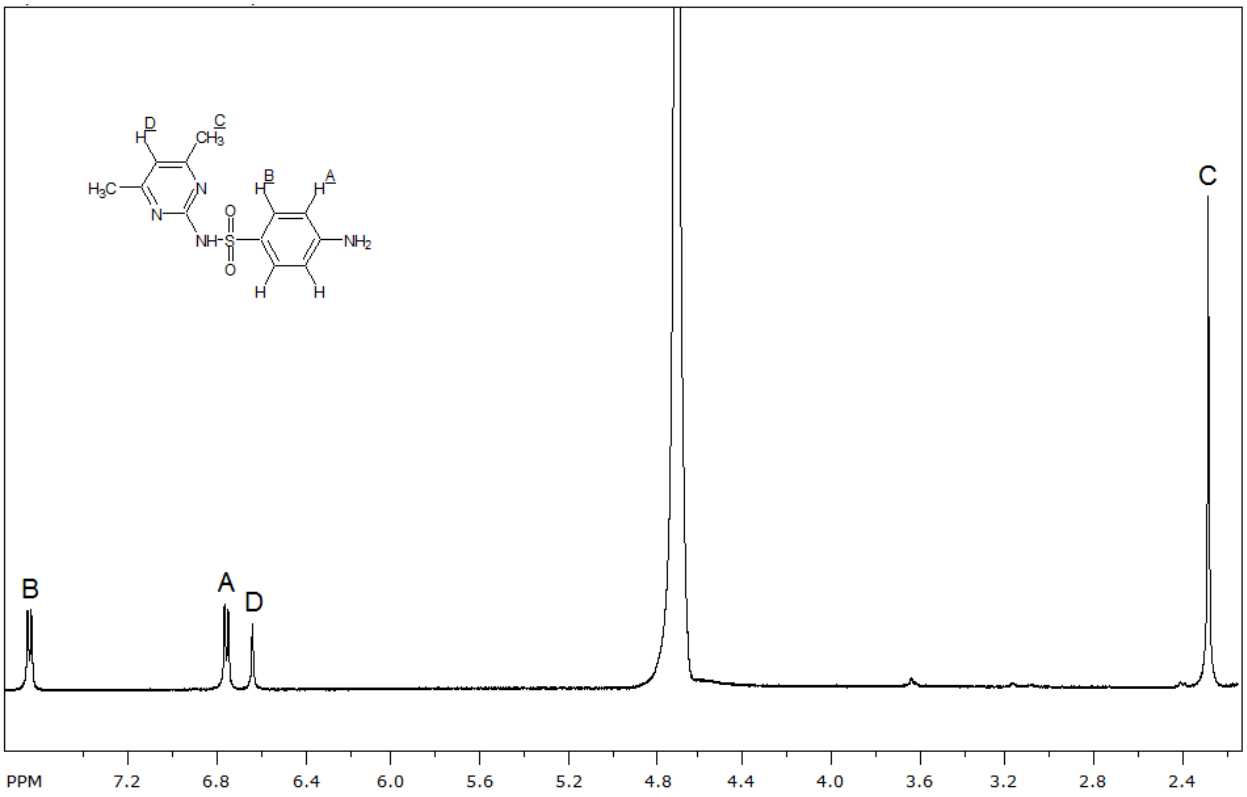

A: δ = 6.763 ppm, d, J_{A-B} = 8.7 Hz

B: δ = 7.662 ppm, d, J_{A-B} = 8.7 Hz

C: δ = 6.645 ppm, s

D: δ = 2.273 ppm, s

Sulfamethoxazole ^{1}H NMR (500 MHz, D_2O)

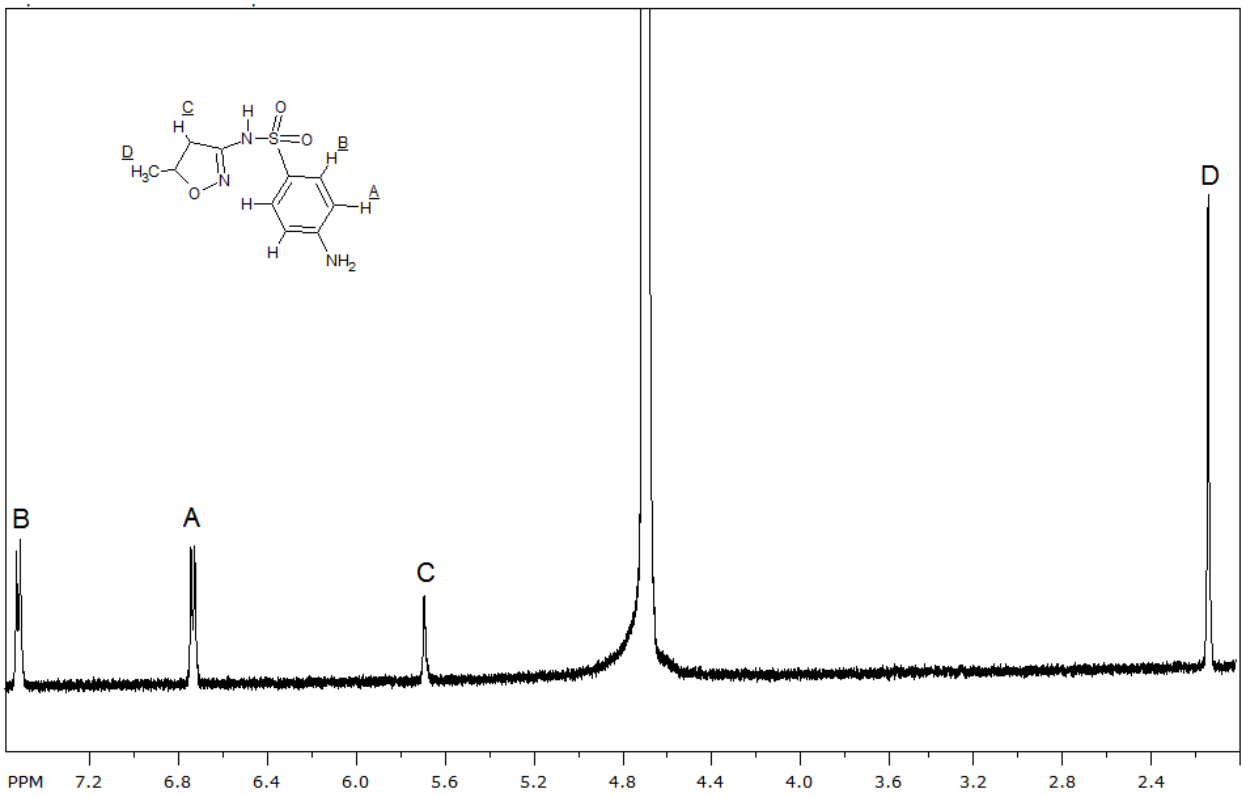

A: δ = 6.745 ppm, d, J_{A-B} = 8.6 Hz

B: δ = 7.535 ppm, d, J_{A-B} = 8.6 Hz

C: δ = 5.697 ppm, s

D: δ = 2.140 ppm, s

Sulfathiazole ^{1}H NMR (500 MHz, D_2O)

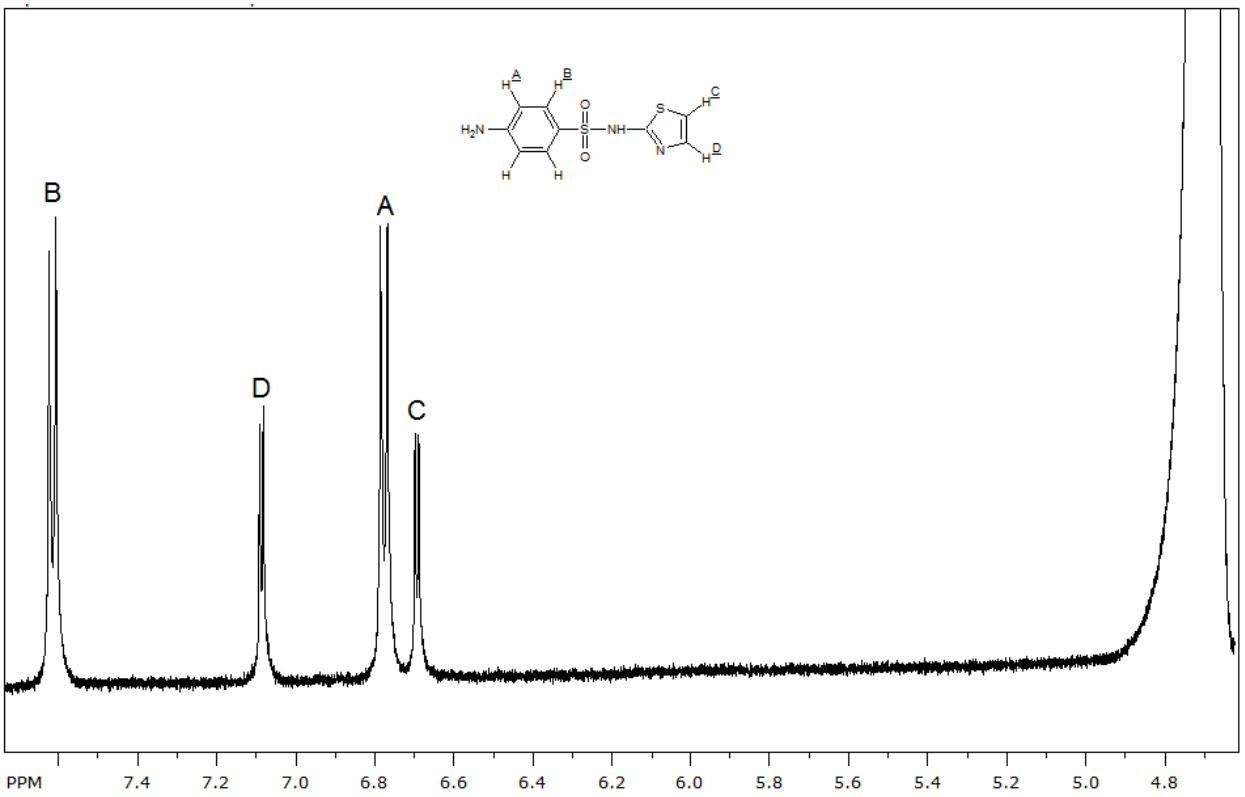

A: δ = 6.777 ppm, d, J_{A-B} = 8.8 Hz

B: δ = 7.616 ppm, d, J_{A-B} = 8.8 Hz

C: δ = 6.694 ppm, d, J_{C-D} = 4.6 Hz

D: δ = 7.087 ppm, d, J_{C-D} = 4.6 Hz

CTABr ^{1}H NMR (500 MHz, D_2O)

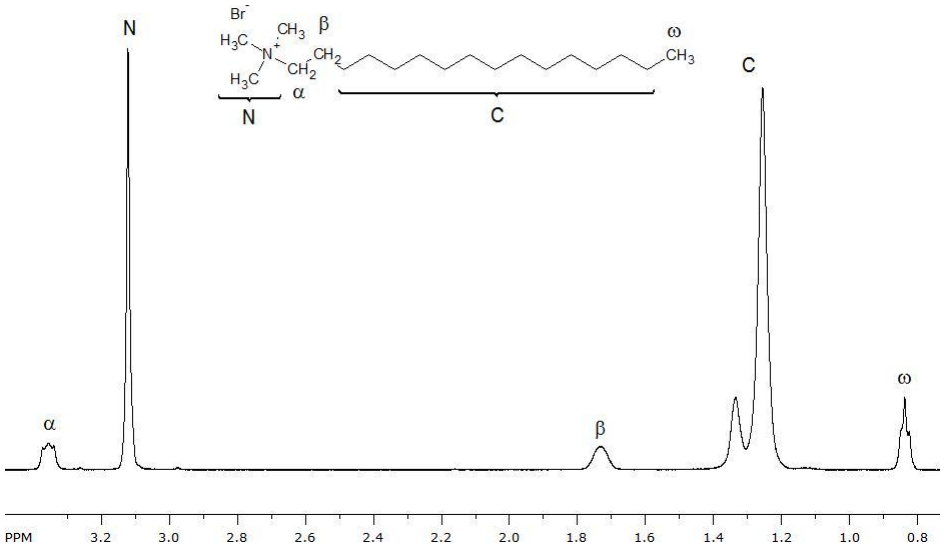

N: δ = 3.117 ppm, s

α: δ = 3.356 ppm, t, $J_{\alpha-\beta}$ = 8.2 Hz

β: δ = 1.721 ppm, m

C: δ = 1.241 ppm, m

ω: δ = 0.823 ppm, m

Appendix B

NMR Binding Curve Derivation

Terms:

C_s = Concentration of Surfactant in Solution

C_{CMC} = Critical Micelle Concentration of Surfactant

δ = Chemical Shift of Atom

δ_o = Chemical Shift of Atom when $C_s = 0$

δ_m = Chemical Shift of Atom when C_s is very large

K_B = Binding Constant

M_V = Molar Volume of Surfactant

$[A]_M$ = Concentration of Analyte in Micelles

$[A]_S$ = Concentration of Analyte in Solution

V_M= Volume of Micelles

V_S= Volume of Solution

Begin by defining equations (1) and (2)

(1) $K_B = \frac{[A]_M}{[A]_S}$

(2) $V_M = M_V(C_S - C_{CMC})V_S$

For the bound fraction, we can say that:

(3) $\frac{\delta-\delta_0}{\delta_M-\delta_0} = \frac{[A]_M V_M}{[A]_S V_S + [A]_M V_M}$

Solving (1) for $[A]_M$ and substituting into (3) yields:

$$\frac{\delta-\delta_0}{\delta_M-\delta_0} = \frac{K_B[A]_S V_M}{[A]_S V_S + K_B[A]_S V_M}$$

(4) $\frac{\delta-\delta_0}{\delta_M-\delta_0} = \frac{K_B V_M}{V_S + K_B V_M}$

Inverting (4) yields:

$$\frac{\delta_M-\delta_0}{\delta-\delta_0} = \frac{V_S+K_B V_M}{K_B V_M}$$

$$\frac{\delta_M-\delta_0}{\delta-\delta_0} = \frac{V_S}{K_B V_M} + 1$$

(5) $\frac{\delta_M-\delta_0}{\delta-\delta_0} = \frac{V_S}{K_B V_M} + \frac{\delta-\delta_0}{\delta-\delta_0}$

Rearranging (5) yields:

$$\frac{\delta_M-\delta_0}{\delta-\delta_0} - \frac{\delta-\delta_0}{\delta-\delta_0} = \frac{V_S}{K_B V_M}$$

(6) $\frac{\delta_M-\delta}{\delta-\delta_0} = \frac{V_S}{K_B V_M}$

Solving for δ yields:

$$\delta_M - \delta = \frac{V_S}{K_B V_M}(\delta - \delta_0)$$

$$\delta = \frac{\delta V_S}{K_B V_M} - \frac{\delta_0 V_S}{K_B V_M} - \delta_M$$

$$\delta\left(\frac{V_S}{K_B V_M} + 1\right) = \frac{\delta_0 V_S}{K_B V_M} + \delta_M$$

$$\delta\left(\frac{V_S+K_B V_M}{K_B V_M}\right) = \frac{\delta_0 V_S+\delta_M K_B V_M}{K_B V_M}$$

(7) $\delta = \frac{\delta_0 V_S+\delta_M K_B V_M}{V_S+K_B V_M}$

Substituting (2) into (7) yields:

$$\delta = \frac{\delta_0 V_S + \delta_M K_B (M_V (C_S - C_{CMC}) V_S}{V_S + K_B (M_V (C_S - C_{CMC}) V_S)}$$

(8) $$\delta = \frac{\delta_0 + \delta_M K_B M_V (C_S - C_{CMC})}{1 + K_B M_V (C_S - C_{CMC})}$$